University of Reading

Attribution of Amazon floods to modes of climate variability: a review

Article

Published Version

Creative Commons: Attribution 4.0 (CC-BY)

Open access

Towner, J., Cloke, H. L. ORCID: https://orcid.org/0000-0002-1472-868X, Lavado, W., Santini, W., Bazo, J., Coughlan de Perez, E. and Stephens, E. M. ORCID: https://orcid.org/0000-0002-5439-7563 (2020) Attribution of Amazon floods to modes of climate variability: a review. Meteorological Applications, 27 (5). e1949. ISSN 1469-8080 doi: 10.1002/met.1949 Available at https://centaur.reading.ac.uk/92510/

It is advisable to refer to the publisher's version if you intend to cite from the work. See Guidance on citing.

To link to this article DOI: http://dx.doi.org/10.1002/met.1949

Publisher: Royal Meteorological Society

All outputs in CentAUR are protected by Intellectual Property Rights law, including copyright law. Copyright and IPR is retained by the creators or other copyright holders. Terms and conditions for use of this material are defined in the End User Agreement.

www.reading.ac.uk/centaur

University of Reading

CentAUR

Central Archive at the University of Reading

Reading's research outputs online

Received: 6 March 2020 | Revised: 31 July 2020 | Accepted: 23 August 2020

DOI: 10.1002/met.1949

REVIEW ARTICLE

Meteorological Applications RMetS

Attribution of Amazon floods to modes of climate variability: A review

Jamie Towner[1] | Hannah L. Cloke[1,2,3,4] | Waldo Lavado[5] | William Santini[6] | Juan Bazo[7,8] | Erin Coughlan de Perez[7,9] | Elisabeth M. Stephens[1]

[1]Department of Geography & Environmental Science, University of Reading, Reading, UK

[2]Department of Meteorology, University of Reading, Reading, UK

[3]Department of Earth Sciences, Uppsala University, Uppsala, Sweden

[4]Centre of Natural Hazards and Disaster Science (CNDS), Uppsala, Sweden

[5]Servicio Nacional de Meteorología e Hidrología, SENAMH, I, Lima, Peru

[6]Géosciences Environnement Toulouse-Observatoire Midi-Pyrénées (GET/OMP), Université Toulouse 3, Toulouse, France

[7]Red Cross Red Crescent Climate Centre, The Hague, the Netherlands

[8]Universidad Tecnológica del Perú (UTP), Lima, Peru

[9]International Research Institute for Climate and Society, Columbia University, Palisades, New York

Correspondence
Jamie Towner, Department of Geography & Environmental Science, University of Reading, Reading RG6 6AB, UK.
Email: j.towner@pgr.reading.ac.uk

Funding information
Natural Environment Research Council, Grant/Award Number: NE/L002566/1

Abstract

Anomalous conditions in the oceans and atmosphere have the potential to be used to enhance the predictability of flood events, enabling earlier warnings to reduce risk. In the Amazon basin, extreme flooding is consistently attributed to warmer or cooler conditions in the tropical Pacific and Atlantic oceans, with some evidence linking floods to other hydroclimatic drivers such as the Madden–Julian Oscillation (MJO). This review evaluates the impact of several hydroclimatic drivers on rainfall and river discharge regimes independently, aggregating all the information of previous studies to provide an up-to-date depiction of what we currently know and do not know about how variations in climate impact flooding in the Amazon. Additionally, 34 major flood events that have occurred since 1950 in the Amazon and their attribution to climate anomalies are documented and evaluated. This review finds that despite common agreement within the literature describing the relationship between phases of climate indices and hydrometeorological variables, results linking climate anomalies and flood hazard are often limited to correlation rather than to causation, while the understanding of their usefulness for flood forecasting is weak. There is a need to understand better the ocean–atmosphere response mechanisms that led to previous flood events. In particular, examining the oceanic and atmospheric conditions preceding individual hydrological extremes, as opposed to composite analysis, could provide insightful information into the magnitude and spatial distribution of anomalous sea surface temperatures required to produce extreme floods. Importantly, such an analysis could provide meaningful thresholds on which to base seasonal flood forecasts.

KEYWORDS

Amazon basin, El Niño Southern Oscillation, floods, hydroclimatic drivers, Madden–Julian Oscillation, river flow

This is an open access article under the terms of the Creative Commons Attribution License, which permits use, distribution and reproduction in any medium, provided the original work is properly cited.
© 2020 The Authors. Meteorological Applications published by John Wiley & Sons Ltd on behalf of the Royal Meteorological Society.

1 | INTRODUCTION

River records highlight that, on average, the Amazon typically experiences an extreme hydrological event (i.e. flood or drought) once *per* decade (Marengo *et al.*, 2011). Yet, since approximately 1990, the flood risk to communities living within the Amazon floodplain is thought to have increased due to a combination of population growth, rapid urban expansion, hydrometeorological change and a possible strengthening of the hydrological cycle (Davidson *et al.*, 2012; Gloor *et al.*, 2013; Filizola *et al.*, 2014; Nobre *et al.*, 2016). Record-breaking floods (e.g. in 2009, 2012, 2014 and 2015) and two "once in a century" droughts recorded in 2005 and 2010 (Marengo and Espinoza, 2016) have demonstrated the significant impact that these events can have on both human and natural systems (Espinoza *et al.*, 2013; Marengo *et al.*, 2013b). The 2012 floods alone affected a reported 202,676 people in Loreto, Peru, with large losses of cropland (about 2,000 ha), an example of the damage inflicted upon livelihoods (IRFC, 2012).

1.1 | Limits and sources of predictability

To provide early flood warnings and consequently reduce risk, the probability of exceeding flood warning thresholds, based on estimates of river discharge produced from global hydrological models (GHMs), can be used (Alfieri *et al.*, 2018). For example, in the Peruvian Amazon, Forecast-based-Financing (FbF), an initiative of the German Red Cross, is being implemented by disaster managers in order to take early action (FbF, 2019). The FbF is a protocol that uses automatic trigger actions (e.g. the delivery of mosquito nets and first-aid kits when a particular magnitude of river discharge is reached) based on probabilistic hydrometeorological forecasts, whereby actions are taken before a flood in order to reduce flood risk (Coughlan de Perez *et al.*, 2015). Currently, the available lead time for skilful forecasts (both weather and hydrological) leaves little time in which to act, particularly when many humanitarian actions require long timescales, such as several weeks ahead to reinforce and modify houses to make them more flood resilient. The ability to predict floods weeks in advance is mainly determined by how the uncertainties in the initial state of the atmosphere and oceans evolve over time (Palmer, 1996). Due to the chaotic nature of the atmosphere, precipitation forecasts that many hydrological models rely upon are typically restricted to lead times up to 15 days ahead (Cloke and Pappenberger, 2009). To overcome this many operational flood forecasting systems (e.g. the Global Flood Awareness System; Alfieri *et al.*, 2013), which provide hydrological forecasts within the Amazon basin, now use ensemble numerical weather predictions (NWPs), commonly referred to as an ensemble prediction system (EPS). Here, the uncertainties in the initial conditions of the deterministic meteorological forecast are represented by perturbing them to produce a range of initial states (commonly between 10 and 51; Emerton *et al.*, 2016). The EPS is then used as an input into a hydrological model to produce a range of river discharge predictions, which are equally probable. Such models typically produce subseasonal forecasts (usually up to 30 days ahead). Monthly and seasonal hydrological forecasts can be achieved in some regions, with several factors influencing the likelihood of a particular atmospheric behaviour occurring (e.g. increased or decreased zonal trade wind speeds). Such factors include anomalous sea surface temperatures (SSTs) (Palmer, 1993; Barnston *et al.*, 1994), vegetation effects (e.g. biotic pump hypothesis; Makarieva and Gorshkov, 2007), land surface anomalies such as soil moisture, surface and groundwater states (Paiva *et al.*, 2012), stratospheric variability (Sigmond *et al.*, 2013), sea-ice and major volcanic events (Robock, 2000).

1.2 | Intensification of the hydrological cycle

When analysing floods, it is important to consider that their frequency and attribution could be related to both the long-term climate signal (e.g. decadal to multidecadal patterns) and to short-term climate variability (e.g. interannual and intra-seasonal patterns). The reported intensification of the hydrological cycle in the Amazon basin with a tendency towards extreme flooding has been associated with a coinciding increasing decadal trend in SSTs in the tropical Atlantic Ocean (+0.7°C between 1990 and 2010; Gloor *et al.*, 2013). Precipitation and consequently river discharge have been found to increase, particularly during the wet season, driving greater difference between peak and minimum flows. Although trends are more dominant in certain regions (e.g. northwestern Amazonia), this intensification is considered for the average trend throughout the entire Amazon, with a greater diversity found in trends of discharge across sub-basins and a large variability is acknowledged in spatial extremes. For example, drying trends are acknowledged in the southern Amazon basin (Espinoza *et al.*, 2009a), with a significant increase in dry day frequency (days with < 1 mm of rainfall; Espinoza *et al.*, 2019). This recent shift in discharge extremes since approximately 1990 is expected to continue in the long term under further atmospheric warming, based on the latest climate projections (Hirabayashi *et al.*, 2013; Langerwisch *et al.*, 2013; Sorribas *et al.*, 2016; Zulkafli *et al.*, 2016; Alfieri *et al.*, 2017). It is important to

consider that any trends and shifts in extremes could be associated with multidecadal natural variability and that projections of future extremes can vary enormously based on different greenhouse gas scenarios, levels of deforestation and other land-use changes, insufficient knowledge on initial and boundary conditions, and model deficiencies in relevant physical processes (Gloor *et al.*, 2013; Torres and Marengo, 2013; Marengo *et al.*, 2018).

1.3 | Hydroclimatic drivers

Climatic or hydroclimatic drivers can be defined as modes of large-scale climate variability around a long-term trend that has the potential to drive spatial and temporal changes in hydrometeorological variables (i.e. precipitation and river discharge; Nobre *et al.*, 2017). To explore such drivers, we first identify using the scientific literature those responsible for impacting atmospheric circulation, moisture transport and thus hydrometeorological variables in and around South America (Table 1). For the Amazon, increased rainfall and river discharge are consistently attributed to lower and upper atmospheric circulation anomalies as a consequence of anomalous SST conditions in the tropical Atlantic and Pacific oceans (Richey *et al.*, 1989; Yoon and Zeng, 2010; Davidson *et al.*, 2012; Marengo and Espinoza, 2016). Other, less studied, climate drivers have also been related to flooding in the Amazon (e.g. the Madden–Julian Oscillation—MJO; Shimizu *et al.*, 2017), with climate variations operating at lower frequencies (e.g. Pacific Decadal Oscillation—PDO; and Atlantic Multidecadal Oscillation—AMO; Barichivich *et al.*, 2018) also linked to wetter and drier conditions. An overview of each driver and their mechanisms are provided in Table 1. Here, general definitions are provided, with their influence on the spatial pattern of Amazon rainfall and river discharge discussed in Section 4.

1.4 | Attribution

Attribution studies attempt to understand to what extent can certain factors (e.g. land cover change, SST anomalies) explain changes in certain variables (e.g. streamflow) or the likelihood or indeed the strength of hydrometeorological events taking place. Attribution encompasses a range of different kinds of studies (e.g. the influence of land-cover changes on streamflow, Slater and Villarini, 2017; urbanisation influence on flooding intensity, Zhang *et al.*, 2018), though two types are particularly common for extreme event attribution. The first type attempts to establish an association between an event and climatological patterns (e.g. floods caused by El Niño). The second type assesses the role of human-induced activities and climate change (e.g. through increased greenhouse gas emissions) on a particular event (Trenberth *et al.*, 2015). In this review we focus on the former. To relate an event to a specific climate pattern, common methods vary from basic correlation analysis, partially linking events and climatic drivers, to the use of climate models and ensemble forecasts to predict the response of the climate to different atmospheric and oceanic forcings (Coumou and Rahmstorf, 2012).

1.5 | From sources of predictability to early warning

Many studies have identified the impacts that different sources of predictability (e.g. SST anomalies) can have on hydrometeorological variables in the Amazon (e.g. Richey *et al.*, 1989; Ronchail *et al.*, 2002; Yoon, 2016; Sulca *et al.*, 2018). Fewer studies, however, demonstrate how knowledge about these relationships can translate into improved flood prediction and risk reduction using early warning systems (EWS). An EWS is a protocol that uses information of potential upcoming natural hazards (e.g. floods), from climate models forced by seasonal forecasts of the SST and other sources of predictability. Such information is then used to help inform decision-making (e.g. whether to distribute water purification tablets or evacuate a particular community) in an attempt to reduce risk before an event taking place (Coughlan de Perez *et al.*, 2015). The EWS combine several disciplines and can generally be described as a chain consisting of four main categories: (1) risk knowledge, (2) monitoring, forecasting and warning, (3) communication of early warning and (4) response capability (Cools *et al.*, 2016). Though many challenges remain to achieve the full benefits of an EWS, particularly with regards to categories 3 and 4 and understanding the feedbacks and interactions between the physical and social systems (Lopez *et al.*, 2017), the evidence required for the forecasting component of the chain remains essential for effective alerts and the communication of early risk information.

Currently, the available evidence demonstrating the potential usefulness of the SST anomalies as predictors for forecasting flood variables in the Amazon comes mainly from statistical modelling, with simulations forced using SST data. For instance, Schöngart and Junk (2007) developed a retrospective forecast model that showed that water levels in central Amazonia were an integrator of Pacific SSTs, with forecasts of water levels achievable up to four months in advance when modelled results were compared with observations for the period 1903–2004. Other studies include the use of a series of statistical models forced by lagged spatial averages of

TABLE 1 Hydroclimatic drivers of Amazon flooding, their description, mechanisms and key references

Hydroclimatic driver	Description	Timescale	Mechanism	Reference(s)
El Niño Southern Oscillation (ENSO)	Set of indices measuring the interannual variability of sea surface temperatures (SSTs) in the Equatorial Pacific Ocean (5° N–5° S, 170–120° W), with oscillating phases of warmer or cooler than usual conditions generated by coupled atmosphere and oceanic interactions. Anonymously warm or cold SSTs are termed El Niño and La Niña events, respectively	Interannual	During El Niño, the lower Equatorial easterly trade winds and surface zonal currents become weaker owing to surface air pressure over the tropical western Pacific becoming higher than in the tropical eastern Pacific relative to mean conditions. Consequently, the upwelling of cold water in the eastern Pacific is reduced, leading to a deeper thermocline and a shift of the warmer SSTs into the eastern and central tropical Pacific. As a result, the Pacific Walker circulation, and hence convective rainfall, also shifts eastwards, impacting rainfall and discharge patterns in the surrounding continents (Yeh *et al*., 2018). During La Niña, the easterly trade winds are enhanced, leading to increased upwelling of cold Pacific waters off the coast of Peru and colder than usual SSTs in the eastern and central tropical Pacific. Rainfall patterns are consequently displaced further west compared with neutral conditions	Bjerknes (1969); Trenberth (1997); Trenberth *et al*. (2001)
Tropical North Atlantic (TNA)	Patterns of average SST variability in the TNA (5.5–23.5° N, 15–57.5° W). Couples with the variability in the Tropical South Atlantic (TSA), influencing the migration pattern of the intertropical convergence zone (ITCZ)	Interannual	When the TNA is abnormally warmer (cooler) than usual, the ITCZ is found to migrate anomalously north (south), bringing changes to low-level atmospheric circulation and spatial rainfall patterns. These patterns are associated with a weakening (intensification) of the northeastern trade winds and moisture flux from the Atlantic basin (Enfield, 1996; Nobre and Shukla, 1996; Panisset *et al*., 2018)	Enfield (1996); Enfield *et al*. (1999)
Tropical South Atlantic (TSA)	Patterns of averaged SST variability in the TSA (Equator–20° S, 10° E–30° W). Couples with the variability in the TNA, influencing the migration pattern of the ITCZ	Interannual	When the TSA is warmer (cooler) than usual, the ITCZ shifts further south (north), weakening (strengthening) the southeast trade winds (Utida *et al*., 2019). Consequently, this changes the location of maximum tropical convection and precipitation, influencing upper and lower flows. The ITCZ commonly reaches its most southernmost position during austral autumn (March–May), when TSA SSTs are at their highest. In contrast, coolest temperatures and a northern migration of the ITCZ are common during austral winter (June–August)	Enfield (1996); Enfield *et al*. (1999)
Madden–Julian Oscillation (MJO)	The dominant component of the intra-seasonal (30–60 days) variability in the tropical atmosphere. The MJO is a	Intra-seasonal (about 30–60 days)	The MJO consists of simultaneous convective and supressed rainfall phases that operate in a dipole structure. The locations of convection are often grouped into eight stages, based on the geographical location (Pohl and	Madden and Julian (1971, 1972, 1994); Zhang (2005)

TABLE 1 (Continued)

Hydroclimatic driver	Description	Timescale	Mechanism	Reference(s)
	moving pattern, propagating eastward through the atmosphere above warm portions of the Indian and Pacific oceans		Matthews, 2007, fig. 1). Events of the MJO force a thermodynamic response in the upper layers of the ocean. When active, the MJO modifies extratropical circulation *via* a Rossby wave response to latent heat release, related to tropical convection (Matthews *et al*., 2004). An enhanced (supressed) convective phase leads to a reduction (increase) in latent heat fluxes and thus cooling (warming) of the SSTs, prompting an eastward propagation (Webber *et al*., 2010). In regions of anomalously warm SSTs, there is increased large-scale ascent and upper tropospheric divergence. In contrast, in locations that lack convective activity, increased descent and upper-tropospheric convergent inflow are witnessed (Matthews *et al*., 2004)	
Pacific Decadal Oscillation (PDO)	Empirical orthogonal function (EOF) of monthly anomalies of the SST in the North Pacific Ocean, poleward of 20° N	Decadal (about 16–20 and 50–70 years)	The physical mechanisms driving the PDO and its variability remain unclear (Mantua and Hare, 2002; Geng *et al*., 2019). Possible explanations argue that oceanic Rossby waves driven by atmospheric forcing are pivotal in maintaining and setting the timescale of the PDO variability (Geng *et al*., 2019). While Newman *et al*. (2016) describe the mechanisms of the PDO as a set of atmospheric–oceanic processes rather than a single mode of climate variability, meaning the PDO impacts stated in the literature may instead represent correlation to processes driving variations in both the PDO and impact variables. The impact of the PDO variability on hydrometeorological variables is locally specific, generally producing similar responses to the ENSO (e.g. the warm PDO impacts are similar to the response to El Niño conditions)	Mantua *et al*. (1997); Zhang *et al*. (1997)
Atlantic Multidecadal Oscillation (AMO)	Oscillation of the SSTs in the North Atlantic Ocean, typically within a 0.4°C range	Multidecadal (about 50–70 years)	Similarly, to the PDO, owing to the relatively short observational record and timescale at which the driver operates, the mechanisms and variability of the AMO are still debated (Wills *et al*., 2019). Previous studies have shown the AMO to be related to heat transport by the Atlantic meridional overturning circulation (AMOC) (Zhang and Wang, 2013), to the variability of aerosol forcing on surface short wave radiation (Booth *et al*., 2012) and due to the low	Kerr (2000)

(Continues)

TABLE 1 (Continued)

Hydroclimatic driver	Description	Timescale	Mechanism	Reference(s)
			frequency forcing of the SSTs, driven by ocean circulation variability (O'Reilly *et al.*, 2016). In the positive (negative) phase, the SSTs are warmer (cooler) in the North Atlantic, whilst being cooler (warmer) in the Equatorial Atlantic (Martin-Rey *et al.*, 2018). Consequently, the mean oceanic and atmospheric states have been found to be significantly different between positive and negative periods (Jones and Carvalho, 2018)	

central and tropical North Atlantic SSTs to explain variability in terrestrial water storage anomalies (De Linage, Famiglietti, & Randerson, 2014) and a statistical model that showed that northern (southern) sub-basins in the Amazon basin are better forecasted when using Pacific (Atlantic) SSTs (Uvo and Graham, 1998).

1.6 | Objective and framework

Having first identified the main hydroclimatic drivers that influence the atmospheric circulation and moisture transport in and around South America (Table 1), the objective of this review is to draw together knowledge of the current understanding of how each driver impacts the characteristics of rainfall and river discharge regimes and their links to extreme flooding in the Amazon basin. Due to the non-linearity between rainfall and river discharge (Stephens *et al.*, 2015), and significant differences previously identified between the mean states of the two variables in response to phases of climatic indices (Dettinger and Diaz, 2000), it is important to consider the effect of large-scale climate variability for each independently. Therefore, the framework of this review is structured based on the discussion of how hydroclimatic drivers influence rainfall variability, river discharge variability and the relationship between previous extreme flood occurrences and different climate phases; thereby scoping out the potential for earlier flood warning in the Amazon basin.

2 | METHODS AND DATA

Using the published literature, the impact of the SST anomalies from different ocean basins on rainfall and river discharge regimes are evaluated across different regions of the Amazon basin. The evaluation is broken down for rainfall and discharge independently and consists of combining the results from previous studies to provide an up-to-date depiction of the current knowledge in the form of composite maps (in Section 4).

To evaluate the relationship between climate phases and extreme flood events, we have constructed a table of major floods as sourced from the scientific literature, humanitarian reports and flood databases (i.e. the Dartmouth Flood Observatory) throughout the Brazilian, Bolivian and Peruvian Amazon since 1950 (Table 2) (see Section 5). While reports of flooding in the Amazon basin date to the mid-19th century (e.g. 1859; Le Cointe, 1935), earlier records are often assembled from qualitative data such as newspapers, humanitarian records and verbal information from communities (Sutcliffe, 1987). In addition, the

TABLE 2 Characteristics of flood events in the Amazon basin and their links to hydroclimatic drivers

Year and location affected	Peak discharge timing	Peak discharge ($m^3 \cdot s^{-1}$)	Days over 90th percentile of flow	Attributed flood driver	EN 3.4 (°C) (October–December/December–February)	MEI v2 EN (°C) (October–December/December–February)	TNA (°C) (March–May)	TSA (°C) (March–May)	Phase of the PDO/AMO (°C)	Method of analysis	Strength of evidence	Reference(s)
1953 Eastern Amazon[b]	–[b]	–[b]	–[b]	Warm TSA	0.05/0.40	–	0.08	−0.14	Cold (−0.57)/ warm (0.26)	None	Very low	**Marengo *et al.* (2013a);** Satyamurty *et al.* (2013); Rodier and Roche (1984); O'Connor and Costa (2004); Callède *et al.* (2004)
1956 Southwest[f]	–[f]	–[f]	–[f]	LN	−1.67/−1.11	–	−0.11	−0.58	Cold (−1.82)/ warm (−0.03)	Correlation analysis between rainfall, inundation and SST	Low	**Ronchail *et al.* (2005a)**
1958 Southwest[f]	–[f]	–[f]	–[f]	EN	1.53/1.80	–	0.85	−0.76	Cold (0.92)/ warm (0.20)	See 1956	Low	**Ronchail *et al.* (2005a)**
1963 Eastern Amazon[b]	–[b]	250,000[*b]	–[b]	Not defined	−0.30/−0.40	–	0.30	0.30	Cold (−0.28)/ warm (−0.01)	No link to hydroclimate drivers	–	Rodier and Roche (1984) O'Connor and Costa (2004)
1966 Southwest[f]	–[f]	–[f]	–[f]	EN	1.97/1.37	–	0.44	−0.06	Cold (−0.50)/ cold (0.00)	See 1956	Low	**Ronchail *et al.* (2005a)**
1968 Southwest[d,h]	25 February 1968[d] 25 February 1968[h]	17,490[d] 17,490[h]	22[d] 22[h]	Non-ENSO	−0.34/−0.63	–	−0.09	−0.09	Cold (−0.19)/ cold (−0.18)	Discharge > 6,000 $m^3 \cdot s^{-1}$ at Rurrenbaque gauging station compared with the ONI ENSO classification	–	Vauchel *et al.* (**2017**); Gautier *et al.* (2006)
1971 Southwest[d,h]	26 February 1971[d] 26 February 1971[h]	17,340[d] 17,340[h]	57[d] 56[h]	LN	−0.86/−1.36	–	−0.33	0.09	Cold (−1.34)/ cold (−0.32)	Discharge > 15,000 $m^3 \cdot s^{-1}$ at Rurrenbaque gauging station compared with the ONI ENSO classification	Low	**Espinoza *et al.* (2014)** Vauchel *et al.* (2017) Gautier *et al.* (2006)

(Continues)

TABLE 2 (Continued)

Year and location affected	Peak discharge timing	Peak discharge ($m^3 \cdot s^{-1}$)	Days over 90th percentile of flow	Attributed flood driver	EN 3.4 (°C) (October–December/December–February)	MEI v2 EN (°C) (October–December/December–February)	TNA (°C) (March–May)	TSA (°C) (March–May)	Phase of the PDO/AMO (°C)	Method of analysis	Strength of evidence	Reference(s)
1972 Southwest[h]	22 January 1972[h]	14,850[h]	16[h]	Not defined	−0.96/−0.70	–	−0.42	−0.06	Cold (−1.17)/cold (−0.37)	No link to hydroclimate drivers	–	Gautier *et al.* (2006)
1973 Eastern Amazon[c] Southwest[d,f]	21 June 1973[c] 29 January 1973[d] –[f]	146,800[c] 12,560[d] –[f]	0[c] 41[d] –[f]	EN	2.09/1.85	–	−0.16	0.76	Cold (−1.18)/cold (−0.23)	See 1956	Low	**Ronchail *et al.* (2005a)** Vauchel *et al.* (2017) Richey *et al.* (1989)
1974 Southwest[d,f,h]	16 January 1974[d] –[f] 16 January 1974[h]	13,290[d] –[f] 13,290[h]	42[d] –[f] 42[h]	LN	−1.95/−1.84	–	−0.90	0.33	Cold (−0.38)/cold (−0.43)	See 1956	Low	**Ronchail *et al.* (2005a)** Vauchel *et al.* (2017) Gautier *et al.* (2006)
1975 Southwest[f]	–[f]	–[f]	–[f]	LN	−0.75/−0.54	–	−0.55	−0.07	Cold (−1.46)/cold (−0.31)	See 1956	Low	**Ronchail *et al.* (2005a)**
1976 Eastern Amazon[b,c]	20 May 1976[b] 26 June 1976[c]	269,400[b] 145,600[c]	81[b] 0[c]	LN	−1.55/−1.55	–	−0.75	−0.62	Cold (−0.18)/cold (−0.39)	Composite analysis of the SST anomalies and moisture flux (October–April) for the five highest flood years before 2012 (1953, 1976, 1989, 1999 and 2009)	Medium	**Satyamurty *et al.* (2013)** Rodier and Roche (1984) Richey *et al.* (1989) O'Connor and Costa (2004)
1977 Southwest[f]	–[f]	–[f]	–[f]	EN	0.86/0.71	–	−0.09	−0.03	Warm (0.02)/cold (−0.20)	See 1956	Low	**Ronchail *et al.* (2005a)**
1978 Southwest[d,f,h]	5 February 1978[d] –[f] 5 February 1978[h]	19,730[d] –[f] 19,730[h]	21[d] –[f] 19[h]	Warm SSA Negative TSA–SSA gradient EN	0.81/0.69	–	0.20	−0.58	Warm (0.01)/cold (−0.19)	Composite analysis of the SST, 850 hPa geopotential height and humidity flux anomalies for non-La Niña	Medium	**Espinoza *et al.* (2014)** **Ronchail *et al.* (2005a)** Gautier *et al.* (2006)

TABLE 2 (Continued)

Year and location affected	Peak discharge timing	Peak discharge ($m^3 \cdot s^{-1}$)	Days over 90th percentile of flow	Attributed flood driver	EN 3.4 (°C) (October–December/December–February)	MEI v2 EN (°C) (October–December/December–February)	TNA (°C) (March–May)	TSA (°C) (March–May)	Phase of the PDO/AMO (°C)	Method of analysis	Strength of evidence	Reference(s)
										floods (1978, 1982, 2001 and 2014) See 1956		
1982 Southwest[d,f,h]	6 March 1982[d] –[f] 6 March 1982[h]	16,720[d] –[f] 16,720[h]	23[d] –[f] 22[h]	Warm SSA Negative TSA–SSA gradient	−0.15/−0.05	−0.17/−0.34	−0.09	−0.31	Warm (−0.25)/ cold (−0.23)	See 1978	Medium	**Espinoza *et al.* (2014)** Gautier *et al.* (2006)
1983 Southwest[f,h]	–[f] 18 February 1983[h]	–[f] 12,700[h]	–[f] 8[h]	EN	2.18/2.18	2.23/2.60	0.35	0.18	Warm (1.19)/ cold (−0.09)	See 1956	Low	**Ronchail *et al.* (2005a)** Gautier *et al.* (2006)
1984 Southwest[d,h]	2 March 1984[d] 2 March 1984[h]	13,100[d] 13,100[h]	64[d] 54[h]	Non-ENSO	−1.00/−0.60	−0.43/−0.49	−0.15	0.52	Warm (0.59)/ cold (−0.22)	See 1968	Low	**Vauchel *et al.* (2017)** Gautier *et al.* (2006)
1986 Peruvian Amazon[a]	8 May 1986[a]	53,920[a]	54[a]	LN	−0.27/−0.49	−0.14/−0.34	−0.60	0.31	Warm (0.96)/ cold (−0.30)	Composite analysis of the SST, 850 hPa geopotential height and humidity flux anomalies for October–December 1985, 1992, 1998 and 2011	Low	**Espinoza *et al.* (2013)**
1989 Peruvian Amazon[a] Eastern Amazon[b]	9 May 1989[a] 6 June 1989[b]	48,220[a] 274,400[b]	3[a] 96[b]	LN	−1.80/−1.69	−1.55/−1.21	−0.74	0.32	Warm (−0.55)/ cold (−0.10)	Comparison of the 1989, 1999 and 2009 floods comparing the	Medium	**Marengo *et al.* (2012)** Satyamurty *et al.* (2013)

(Continues)

TABLE 2 (Continued)

Year and location affected	Peak discharge timing	Peak discharge ($m^3 \cdot s^{-1}$)	Days over 90th percentile of flow	Attributed flood driver	EN 3.4 (°C) (October–December/December–February)	MEI v2 EN (°C) (October–December/December–February)	TNA (°C) (March–May)	TSA (°C) (March–May)	Phase of the PDO/AMO (°C)	Method of analysis	Strength of evidence	Reference(s)
										atmospheric and SST anomalies and further hydrological analysis (e.g. mean and maximum Q/timing of Q)		
1992 Southwest[f]	–[f]	–[f]	–[f]	MEI EN	1.21/1.71	1.18/1.53	−0.22	−0.54	Warm (0.70)/ cold (−0.23)	See 1956	Low	**Ronchail *et al.* (2005a)** Bourrel *et al.* (2009)
1993 Peruvian Amazon[a] Eastern Amazon[b] Southwest[f]	11 May 1993[a] 23 May 1993[b] –[f]	51,740[a] 246,000[b] –[f]	64[a] 61[b] –[f]	LN MEI EN	−0.28/0.09	0.75/0.83	−0.11	0.05	Warm (0.97)/ cold (−0.23)	See 1986 See 1956	Low	**Espinoza *et al.* (2013)** **Ronchail *et al.* (2005a)** Bourrel *et al.* (2009)
1994 Southwest[i]	–[i]	–[i]	–[i]	Not defined	0.04/0.06	0.63/0.04	−0.52	0.18	Warm (−0.53)/ cold (−0.19)	Hydrological and remote sensing analysis (discharge and flood imagery) No connection to hydroclimate drivers stated or analysed	–	Bourrel *et al.* (2009)
1995 Southwest[i]	–[i]	–[i]	–[i]	Not defined	1.00/0.96	1.10/0.70	0.12	0.65	Warm (0.32)/ warm (0.12)	See 1994	–	Bourrel *et al.* (2009)
1997 Southwest[f,i]	–[f] –[i]	–[f] –[i]	–[f] –[i]	Not defined	−0.45/−0.50	−0.37/−0.61	0.28	−0.50	Warm (1.22)/ warm (0.03)	See 1994	–	Bourrel *et al.* (2009)

TABLE 2 (Continued)

Year and location affected	Peak discharge timing	Peak discharge ($m^3 \cdot s^{-1}$)	Days over 90th percentile of flow	Attributed flood driver	EN 3.4 (°C) (October–December/December–February)	MEI v2 EN (°C) (October–December/December–February)	TNA (°C) (March–May)	TSA (°C) (March–May)	Phase of the PDO/AMO (°C)	Method of analysis	Strength of evidence	Reference(s)
1998 Southwest[i]	–[i]	–[i]	–[i]	Not defined	2.40/2.24	2.06/2.24	0.64	0.59	Cold (−0.45)/warm (0.36)	See 1994	–	Bourrel *et al.* (2009)
1999 Peruvian Amazon[a] Eastern Amazon[b] Southwest[d,h]	21 May 1999[a] 2 June 1999[b] 20 March 1999[d] 20 March 1999[h]	53,020[a] 268,200[b] 22,330[d] –[h]	54[a] 57[b] 36[d] –[h]	LN	−1.48/−1.55	−1.24/−1.22	−0.08	0.44	Cold (−1.78)/warm (0.10)	See 1986 See 1989	Medium	**Espinoza *et al.* (2013)** **Marengo *et al.* (2012)** Marengo & Espinoza (2016) Gautier *et al.* (2006) Dartmouth Flood Observatory (2018) Vauchel *et al.* (2017)
2001 Southwest[d,h]	13 January 2001[d] 13 January 2001[h]	16,950[d] –[h]	40[d] –[h]	Warm SSA	−0.75/−0.68	−0.76/−0.83	0.09	0.38	Cold (−1.13)/warm (0.10)	See 1978	Medium	**Espinoza *et al.* (2014)** Gautier *et al.* (2006) Vauchel *et al.* (2017)
2007 Southwest[g]	28 April 2007[g]	18,950[g]	40[g]	EN	0.90/0.71	0.73/0.53	0.31	0.19	Cold (−0.78)/warm (0.13)	Hydrological comparison of the 2007, 2008 and 2014 floods (e.g. monthly rainfall and discharge, flood timing, total flooded area based on remote sensing imagery No atmospheric analysis performed	Low	**Ovando *et al.* (2016)** CEPAL (2008) Dartmouth Flood Observatory (2018)
2008 Southwest[g]	18 April 2008[g]	22,620[g]	59[g]	LN	−1.55/−1.59	−1.16/−1.19	0.21	0.69	Cold (−1.75)/warm (0.12)	See 2007	Low	**Ovando *et al.* (2016)** CEPAL (2008) Dartmouth Flood Observatory (2018)

(Continues)

TABLE 2 (Continued)

Year and location affected	Peak discharge timing	Peak discharge ($m^3 \cdot s^{-1}$)	Days over 90th percentile of flow	Attributed flood driver	EN 3.4 (°C) (October–December/ December–February)	MEI v2 EN (°C) (October–December/ December–February)	TNA (°C) (March–May)	TSA (°C) (March–May)	Phase of the PDO/AMO (°C)	Method of analysis	Strength of evidence	Reference(s)
2009 Eastern Amazon[b]	5 August 2009[b]	262,400[b]	50[b]	Warm TSA	−0.60/−0.80	−1.06/−0.97	−0.29	0.62	Cold (−1.09)/ warm (0.02)	See 1989	Medium	**Marengo *et al.* (2012)** Sena *et al.* (2012) Filizola *et al.* (2014)
2011 Southwest[d]	23 February 2011[d]	20,250[d]	38[d]	LN	−1.69/−1.36	−2.03/−1.78	0.38	0.50	Cold (−1.91)/ warm (0.09)	See 1971	Medium	**Espinoza *et al.* (2014)** Vauchel *et al.* (2017)
2012 Peruvian Amazon[a] Eastern Amazon[b]	20 April 2012[a] 18 July 2012[b]	55,400[a] 260,100[b]	70[a] 50[b]	LN + warm TSA	−1.14/−0.82	−1.26/−0.99	−0.11	−0.15	Cold (−1.66)/ warm (0.20)	See 1986 Anomalies also calculated solely for the 2012 event	High	**Espinoza *et al.* (2013)** Marengo & Espinoza (2016) Satyamurty *et al.* (2013)
2014 Southwest[d,e,g]	12 February 2014[d] 30 March 2014[e] 5 April 2014[g]	25,060[d] 59,080[e] 29,090[g]	53[d] 111[e] 85[g]	Warm IP and SSA Negative TSA–SSA gradient	−0.22/−0.37	−0.23/−0.43	−0.21	0.31	Warm (0.48)/ warm (0.09)	See 1978 Anomalies also calculated solely for the 2014 event	High	**Espinoza *et al.* (2014)** Espinoza *et al.* (2012) Ovando *et al.* (2016)
2015 Peruvian Amazon[a]	25 April 2015[a]	53,880[a]	91[a]	Not defined	0.59/0.60	0.25/0.2	−0.09	0.35	Warm (0.92)/ warm (0.10)	None	–	SO-HYBAM (2015)

Notes: The attributed flood driver and method of analysis for each event are taken from the reference(s) highlighted in bold. The SSTs provided are anomalies. Superscripted letters correspond to the gauging stations at which the flood was recorded.

[a]Tamshiyacu, Solimões River (1986–2017).
[b]Óbidos, Amazon River (1968–2018).
[c]Manacapurú, Solimões River (1968–2017).
[d]Rurrenbaque, Beni River (1968–2016).
[e]Porto Velho, Madeira River (1968–2017).
[f]Puerto Varador, Mamoré River (data not available).
[g]Guajara-Mirim, Mamoré River (1971–2014).
[h]Angosto del Bala, Beni River (1968–1994).
[i]Puerto Almacen, Ibaré River (data not available).

LN: La Niña; IP: Indo-Pacific Ocean; SSA: Subtropical South Atlantic; TSA: Tropical South Atlantic.

Sources: Extended table from Marengo and Espinoza (2016). Peak discharges marked with an asterisk (*) are based on those of Rodier and Roche (1984).

reliability and quantity of pressure and SST observations are considered questionable before 1950 (Bunge and Clarke, 2009), and thus we only consider events that have occurred after this period.

Table 2 extends the work of Marengo and Espinoza (2016) to include areas of the Bolivian Amazon, further flooding in the Peruvian and Brazilian Amazon, and an indication of how strong are the links between floods and climate anomalies. The strength of evidence is evaluated as either very low, low, medium or high and considers the magnitude of the SST anomalies, peak river flows, the timing and duration of flood events, how each flood is classified by the authors (e.g. events could be determined by a specific streamflow exceedance), and by the type of analysis performed (e.g. correlation or composite analysis).

A very low rating may be given when observed SST anomalies disagree with the phase of climate variability attributed (e.g. observed positive SST anomalies in the Pacific with a La Niña attribution). A low to medium rating is when SST anomalies are in agreement, but where no atmospheric analysis (e.g. atmospheric response to abnormal SST anomalies) has been performed. Finally, a high rating is when SSTs are highly abnormal, the level of flooding is highly anomalous and the atmospheric response during the event has been inspected for that given year. We consider all major flood events as determined by the reference(s). The stated climate driver for each event and type of analysis performed is obtained from the authors highlighted in bold in Table 2.

2.1 | River discharge data

Peak river flows for floods are obtained from the time series of seven hydrological gauges provided by the national meteorological and hydrological services of the respective countries situated in the Amazon basin and from the Institute of Research for Development (IRD). These include: the Agência Nacional de Águas (Water National Office—ANA, Brazil) and the Servicio Nacional de Meteorología e Hidrología (National Meteorology and Hydrology Service—SENAMHI, Peru and Bolivia). Data are sourced through the SO-HYBAM observational service (see https://hybam.obs-mip.fr/). The locations of stations are displayed in Figure 1, with letters corresponding to each station highlighted throughout the main text to allow for easier interpretation and navigation. The Puerto Varador (f) and Puerto Almacen gauging stations (i) are no longer operational with previous data suffering from uncertainty due to the backwater effect (Meade *et al*., 1991). Therefore, we have excluded discharge information for these stations in Table 2.

2.2 | SST data

Equatorial Pacific SST data are provided by the National Oceanic and Atmospheric Administration's (NOAA) Climate Prediction Centre (CPC), using the monthly ERSSTv5 (centred base periods) Niño 3.4 (5° N–5° S, 170–120° W) data set, which is used as input to the Oceanic Niño Index (ONI). Atlantic SSTs are provided by the Tropical North (5.5–23.5° N and 15–57.5° W) and South (Equator–20° S and 10° E–30° W) Atlantic indices (climatology is 1971–2000; Enfield *et al*., 1999).

The latest version of the Multivariate El Niño Southern Oscillation index (MEI v2), based on five variables (sea level pressure (SLP), SST, surface zonal winds (U), surface meridional winds (V) and outgoing long wave radiation (OLR)) is used to provide an index based on both oceanic and atmospheric conditions from 1979 onwards. It builds on the original MEI index (Wolter and Timlin, 1993) using the JRA-55 global reanalysis (Kobayashi *et al*., 2015). Here, monthly values are based on bimonthly means; for example, August 2018 is calculated from July–August 2018 SST data. In Table 2, MEI values are averaged for three consecutive bimonthly readings. For example, for October–December considering a flood event in 2012, the average is taken from bimonthly values in September–October, October–November and November–December 2011.

The monthly PDO time series, defined as the leading principal component (PC) of monthly anomalies in the North Pacific Ocean, poleward of 20° N (1854–present) is provided by the National Centre for Environmental Information (NCEI). The NCEI PDO index is based on NOAA's extended reconstruction of the SSTs (ERSSTv4). Finally, monthly detrended AMO data are provided by NOAA's ESRL based on the unsmoothed Kaplan SST V2 data set (Enfield *et al*., 2001). The PDO and AMO data in Table 2 are averaged for the calendar year.

3 | THE AMAZON BASIN

The Amazon (Figure 1) is the world's largest river basin, draining an area of approximately 6 million km^2. Its river network consists of over 1,000 tributaries with the main stem discharging an average of about 209,000 m^3·s^{-1} of freshwater into the Atlantic Ocean *per* annum (Molinier *et al*., 1996; Callède *et al*., 2010). The basin extends between 5° N and 20° S, covering seven countries: Brazil (63%), Peru (16%), Bolivia (12%), Colombia (6%), Ecuador (2%), and Venezuela and Guyana (1%) (Espinoza *et al*., 2009b). In terms of climate, the Amazon basin witnesses a large interannual variability of rainfall with distinct spatial variations (see Laraque *et al*., 2007 for

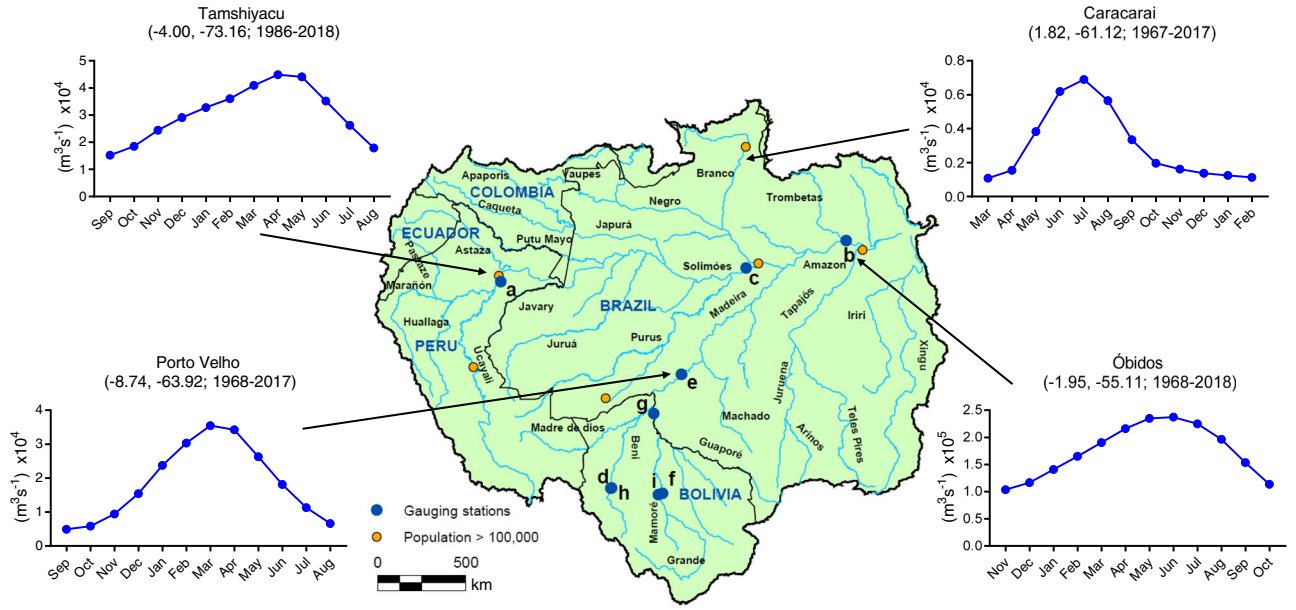

FIGURE 1 River network and hydrographs at key gauging stations within the Amazon basin. Hydrographs show observed mean monthly river flows. The hydrological years for each hydrograph start from the lowest monthly discharge and thus differ depending on the specific station. Letters correspond to the gauging stations used for the classifications of flood events in Table 2 (section 5) and are referred to throughout the main text. City population data are sourced from Esri (https://hub.arcgis.com/)

Ecuador; Ronchail and Gallaire, 2006 for Bolivia; Lavado *et al*., 2012, 2013, for Peru; Figueroa and Nobre, 1990; Ronchail *et al*., 2002, and Espinoza *et al*., 2009b, for the entire Amazon). On average, locations within the Amazon receive around 2,000–2,200 mm of rainfall annually (Marengo and Nobre, 2001), sourced from local evapotranspiration and *via* water transport provided by the easterly trade winds from the Northern Hemisphere (Salati *et al*., 1979; Salati and Vose, 1984). A climatic gradient can be identified from the wet northwest to the dry southern and eastern borders, which experiences a long dry season, and where deforestation from tropical forest to pasture and cropland is at its greatest (Davidson *et al*., 2012).

Owing to the size and location of the basin, both precipitation and discharge regimes differ depending on location. In general, the wet season in the Amazon is from December to April, while its dry period is between June and October (Yoon and Zeng, 2010). More specifically, in the north of the basin, around the Branco catchment (Figure 1), peak rainfall is noted during June–August and is predominately controlled by large-scale convection, modulated by the migration pattern of the intertropical convergence zone (ITCZ) (Ronchail *et al*., 2002). Rainfall totals are greatest near the mouth of the Amazon River within regions of the Amazon Delta and in the northwest towards the Colombian Amazon (Espinoza *et al*., 2009b). In these regions, wetter conditions are prevalent between December and May, though less seasonal variability exists in western catchments (Figueroa and Nobre, 1990; Ronchail *et al*., 2002). Rainfall in the south is heavily influenced by organised convection from the South Atlantic convergence zone (SACZ) and precedes northern regions by approximately six months, peaking in December–February (Ronchail *et al*., 2002; Tomasella *et al*., 2011). Consequently, river discharge in northern, southern and central tributaries also adheres to an asynchronous pattern in peak river flows, providing a dampening effect on the main flood wave travelling down the central Amazon River (Ronchail *et al*., 2006; Espinoza *et al*., 2009a). The rainfall–runoff relationship displays a large lag between peaks in rainfall and peaks in river discharge in large parts of the basin, with river flows showing a stronger response to seasonal rainfall patterns as opposed to single rainfall events (Trigg, 2010). This lag can be related to (1) the size and length of many Amazonian rivers; (2) floodplain storage and interactions; and (3) rivers generally having a shallow bed and topographical slopes, with relatively slow moving waters (Trigg *et al*., 2009; Yamazaki *et al*., 2012), though rivers located in upstream catchments, particularly those of Andean origin, are prone to flash flooding and are highly sensitive to extreme rainfall (Laraque *et al*., 2009). On average, the highest water levels are found two to three months earlier in the largest southern tributary (Madeira River) than its northern counterpart (Rio Negro) and larger tributaries follow a monomodal pattern (i.e. one annual flood wave) (Ronchail *et al*., 2006; Espinoza *et al*., 2009a).

4 | INFLUENCE OF HYDROCLIMATIC DRIVERS

4.1 | Rainfall variability

4.1.1 | Pacific influence

The SST variability in the Equatorial tropical Pacific (i.e. the El Niño Southern Oscillation—ENSO) is arguably the most well-known mechanism responsible for the interannual and spatial variability of Amazon rainfall (Marengo, 1992; Nobre and Shukla, 1996; Foley *et al*., 2002; Espinoza *et al*., 2009b) and indeed worldwide (Cai *et al*., 2015). Figure 2 summarises the relationship between the two phases of the ENSO and Amazon rainfall based on results identified in previous studies. In general, when El Niño (i.e. the warm phase of the ENSO) conditions are prevalent, a deficit in rainfall is common throughout much of the Amazon Basin, whilst the opposite is true for La Niña events (Ronchail *et al*., 2002; Yoon and Zeng, 2010) (Figure 2a,d). This is also evident when examining extreme precipitation frequency, whereby Grimm and Tedeschi (2009) note decreased (increased) activity associated with El Niño (La Niña) conditions over the entire Amazon basin relative to neutral conditions in the austral autumn (March–May). By categorising the wet and dry seasons into dry, very dry, wet and very wet years, based on monthly observed rainfall data (1931–1996), Andreoli *et al*. (2012) showed that dry and very dry rainy seasons are associated with weak and intense El Niño events, respectively. In contrast, very wet rainy and very wet dry seasons are associated with intense La Niña and La Niña conditions.

Rainfall anomalies associated with the ENSO are strongest during the austral summer (December–February) and autumn (March–May), aligning with the peak rainy season in South America (Sulca *et al*., 2018). This is highlighted in Figure 2b,e, where Pacific SST anomalies are found to have a similar influence on annual and wet season (December–April) rainfall patterns. The influence on the dry season (June–October) is more limited, with impacts mainly observed in northern and eastern areas (Figure 2c,f) when using gauge-based rainfall estimation products (Yoon and Zeng, 2010). Investigations performed solely using precipitation observations show contrasting rainfall anomalies between the northern Branco basin and in the southern Amazon during June–August (Ronchail *et al*., 2002) (Figure 2f). During La Niña years, drier-than-usual conditions are more common in the southern Amazon, with wetter conditions in the far north. Here, it is worth reiterating that rainfall in the northern Branco basin generally peaks later (June–August) relative to the rest of the Amazon.

In northern and northeastern catchments of the Brazilian Amazon, the ENSO–rainfall relationship is strong, particularly around the Amazon River towards its mouth on the Atlantic on both annual and seasonal timescales (Liebmann and Marengo, 2001; Ronchail *et al*., 2002; Zeng *et al*., 2008; Yoon and Zeng, 2010). A deficit (increase) in rainfall is recorded at the majority of meteorological stations during El Niño (La Niña) events with a reduction in signal towards southern areas (Ronchail *et al*., 2002; Espinoza *et al*., 2009b). This signal is also identifiable on the western side of the Colombian Andes and Amazon basin, albeit weaker, where abundant rainfall is associated with La Niña conditions (Poveda and Mesa, 1993; Poveda *et al*., 2011; Espinoza *et al*., 2009b) (Figure 2d,e).

For the Peruvian Amazon, particularly areas around Iquitos (a), lower (greater) than usual rainfall is generally associated with El Niño (La Niña) events (Lavado *et al*., 2013; Sulca *et al*., 2018). However, correlations at this station are often weak, with certain analysis having identified both a wet and a dry signal during the warm phase of the ENSO (Ronchail *et al*., 2002; Lagos *et al*., 2008) (Figure 2b). The association between rainfall and the ENSO in the Ecuadorian Amazon is much less well understood owing to its remoteness. Previous studies have mainly focused on the ENSO connection in coastal and Andean locations of Ecuador (Rossel, 1997), with research most likely limited for the Ecuadorian Amazon owing to its remote location and sparse population (Laraque *et al*., 2007). Evidence is conflicting between studies with above-normal rainfall identified during phases of El Niño in the Ecuadorian lowlands and on the eastern slope of the Andes for Ronchail *et al*. (2002), while a deficit in rainfall is acknowledged by Vuille *et al*. (2000), and no significant effect was identified by Tobar and Wyseure (2018) (Figure 2a). The wet signal identified by Ronchail *et al*. (2002) is deemed more significant during the wet season (March–May) (Figure 2b).

The relationship can be complex, particularly when investigating the influence of the ENSO at smaller scales in which distinct spatial differences can be identified. For instance, in Bolivia, correlations are often dependent on altitude and topography (Ronchail and Gallaire, 2006). Less rainfall is reported during the peak of the wet season (February) in the lowlands of the central Bolivian Amazon when La Niña conditions prevail (Trinidad station) (Figure 2e). In contrast, on the slopes of the Zongo Valley, in which the Zongo River empties into the Beni River, an Amazon tributary, drier conditions are reported during El Niño events on an annual time scale, with a La Niña/wet signal evident for February (Ronchail and Gallaire, 2006). This is supported by increased sedimentation within the Beni River during La Niña events (Aalto

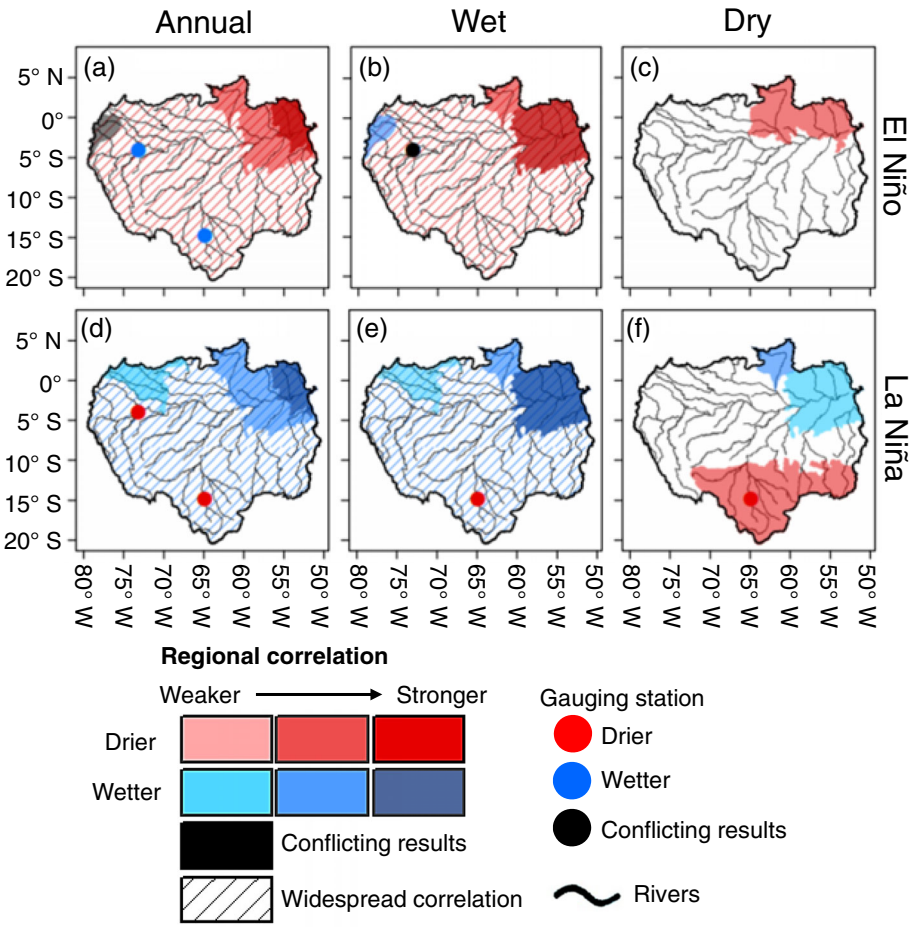

FIGURE 2 Influence of the El Niño Southern Oscillation (ENSO) on rainfall throughout the Amazon basin, based on results identified within the literature: (a, d) the entire year; (b, e) the Amazon wet season (December–April); and (c, f) the Amazon dry season (June–October). Blue circles and shading indicate wetter than usual conditions; red represents drier conditions; black circles or shading are used where conflicting results are found between different authors; darker shading depicts locations where the correlation is considered stronger; regions in white indicate that no correlation exists or that there is currently no information available. Hatched markings highlight when correlations are widespread throughout the majority of the basin. It is important to highlight where widespread correlation is shown, the correlation is not uniform and can be higher or lower for different regions. For full details of the reference(s), type of analysis used and strength of the relationships, see Tables S1–S6 in the additional supporting information

et al., 2003). These findings demonstrate the need to consider the hydrological response to climate anomalies not only at the location of interest but also at locations further upstream owing to increases in river flow in upstream tributaries having the potential to cause flooding further downstream.

Several studies have highlighted the importance of considering the diversity of the ENSO events, with the location and intensity of the SST anomalies in the tropical Pacific found to cause significant differences in rainfall anomalies over South America (Hill *et al*., 2009; Sulca *et al*., 2018; Cai *et al*., 2020). This is a consequence of modifications to the Walker Circulation owing to whether the centre of warming or cooling of the SST anomalies was located in the central or eastern Pacific Ocean (Cai *et al*., 2020). For instance, Sulca *et al*. (2018) identified that a warm eastern Pacific ENSO index results in significant dry anomalies over the Peruvian Amazon, along the Peru–Brazil boundary. These signals were deemed insignificant when the extreme 1983 and 1998 El Niño years were removed, while the dry anomalies were still significant after the removal of these years for the central Pacific index. Such results highlight the need to consider both the SST magnitude and location when attempting to understand the relationship between the ENSO phases and the response of rainfall in different regions of the Amazon basin.

4.1.2 | Atlantic influence

In the early 1990s, Marengo (1992) identified that an increase in rainfall over the Amazon basin was associated with an increase in water vapour fluxes from the Atlantic Ocean. At the time, little attention had been paid to the relationship between the tropical SSTs in the Atlantic and Amazon rainfall. Previous studies mainly focused on the role of Atlantic SSTs in determining rainfall variability over South America, particularly in northeastern Brazil (Moura and Shukla, 1981; Nobre and Shukla, 1996). At the turn of the millennium, Liebmann and Marengo (2001) and Ronchail *et al*. (2002) began to assess the importance of the tropical Atlantic SSTs for the Amazon. However, it was not until after the record-breaking drought event witnessed in 2005 that the tropical Atlantic was considered as a climatic driver, with numerous studies then highlighting the importance of the SST abnormalities in determining the Amazon's water budget (Marengo

et al., 2008; Zeng *et al.*, 2008; Yoon and Zeng, 2010). Generally, more (less) rainfall in the Amazon basin is correlated to anomalously cold (warm) SST conditions in the Tropical North Atlantic (TNA), coupled with warm (cold) SST anomalies in the Tropical South Atlantic (TSA) (Yoon, 2016), associated with the north–south migration pattern of the ITCZ (Enfield, 1996). This is supported by Andreoli *et al.* (2012) who identified that years that are considered to have a drier rainy season are associated with positive (negative) TNA (TSA) SST anomalies. In contrast, a very wet rainy season and wet dry season were associated with the opposite dipole pattern (i.e. a cold TNA and a warm TSA).

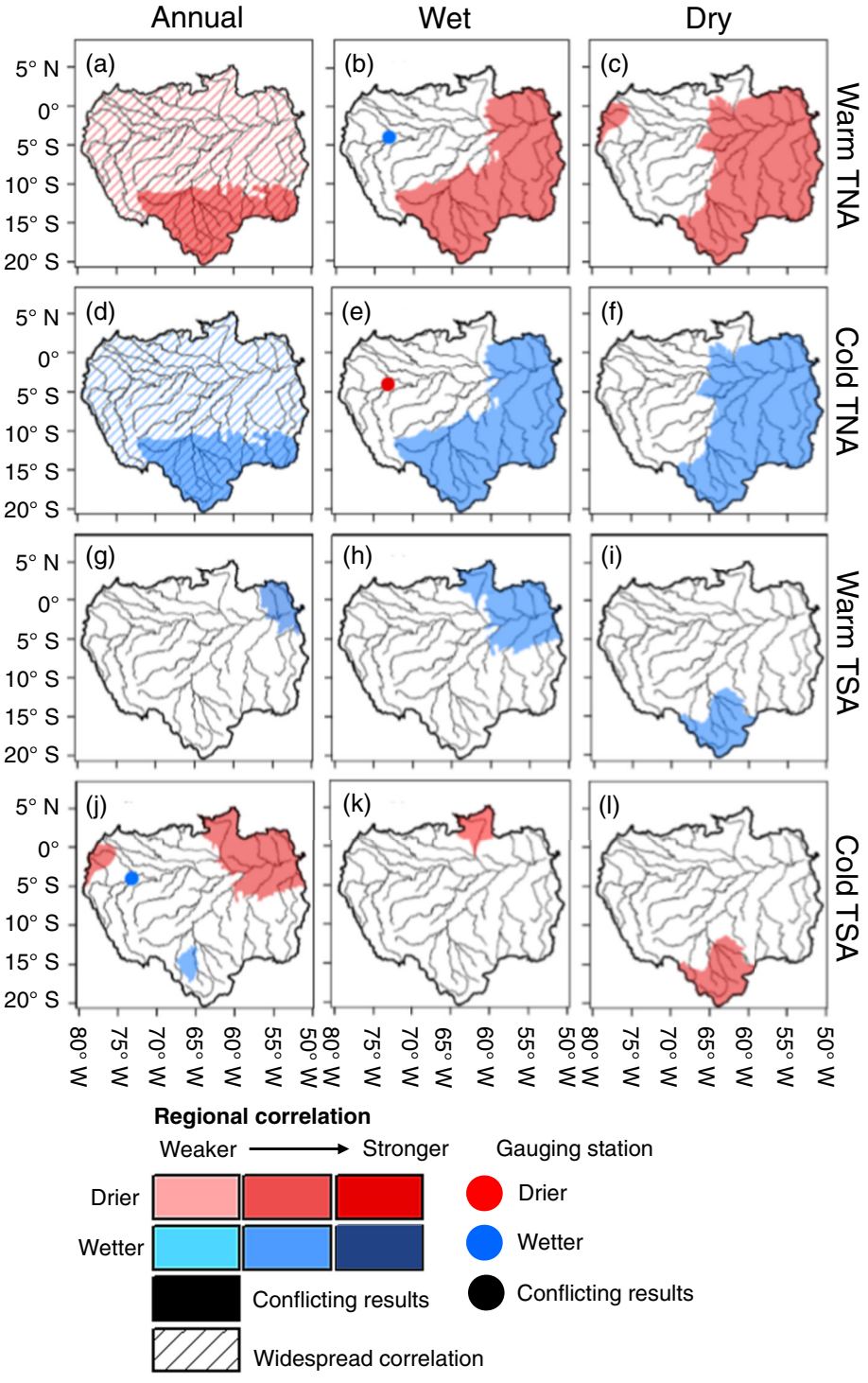

FIGURE 3 Influence of tropical Atlantic sea surface temperatures (SSTs) on rainfall throughout the Amazon basin based on results identified within the literature: (a–c) a warm Tropical North Atlantic (TNA), (d–f) a cold TNA, (g–i) a warm Tropical South Atlantic (TSA) and (j–l) a cold TSA. The legend is the same as for Figure 2. For full details of the reference(s), type of analysis used and strength of the relationships, see Tables S7–S18 in the additional supporting information

Figure 3 provides a summary of how anomalous SSTs in the TNA and TSA affect precipitation variability over the Amazon basin. For the TNA, significant correlations exist over much of the Amazon with a stronger relationship found in the southern Amazon (Zeng *et al.*, 2008; Yoon and Zeng, 2010) (Figure 3a–c). Here, lower than usual precipitation is a persistent response to the warm TNA SST anomalies throughout most of the Amazon basin and is related to a weakening of the northeast trade winds and moisture fluxes towards the basin. This weakening is a result of a northward displacement of the ITCZ, which consequently produces atmospheric subsidence over the Amazon basin (Cox *et al.*, 2008; Marengo *et al.*, 2016). These findings were replicated by Yoon (2016) in an idealised analysis using five atmospheric global climate models (AGCMs). All models were found to simulate drier (wetter) conditions during the dry season in the southern Amazon when SSTs in the north Atlantic were warmer (cooler) than usual. Yoon (2016) highlighted the importance of models accurately representing climatological seasonal rainfall totals in order better simulate the response to anomalous SSTs. Models that simulated too little rainfall during the Amazon dry season tended to underestimate the response to changes to the Atlantic SSTs. When focusing on two of the strongest warm TNA events (2005 and 2010), a contrast in rainfall anomalies is found during March–May, with wetter conditions in the north and drier conditions over the southern Amazon (Jimenez *et al.*, 2019). In the case of 2010, an El Niño event occurred previous to the warm TNA event in March–May, and widespread precipitation deficits were observed over northern Amazonia during December–February, highlighting the need to consider the effects of a combination of climatic phases occurring within a small timeframe.

The TSA, on the other hand, is considered less influential (Figure 3g–l), with its effect more pronounced on the southern edge of the Amazon between June and October (Figure 3l) and during the transitional phase in between the wet and dry seasons (Yoon and Zeng, 2010). Significant correlations do exist between rainfall anomalies and the SSTs in the TSA when analysing correlations against observed rainfall data (Ronchail *et al.*, 2002). For example, when the TSA is warmer than usual, there is a corresponding increase in rainfall at stations located in the northeastern Amazon (Figure 3g).

4.1.3 | Madden–Julian oscillation (MJO)

Unlike the ENSO and tropical Atlantic indices, which typically occur on an interannual timescale, the MJO is an intra-seasonal oscillation, meaning it can occur between seasons in a single year, and it has the potential to provide predictability of rainfall and river discharge for the upcoming season. On a global scale, the MJO is considered the greatest modulator of regional rainfall on an intra-seasonal timescale, and is particularly influential in parts of the eastern Amazon (De Souza and Ambrizzi, 2006). Jones *et al.* (2004) identified that when convective activity was enhanced over the western Indian Ocean, there was an increase in the frequency of precipitation extremes in the eastern part of South America. The reasoning behind this increase has been associated with increased activity and rainfall within the SACZ, whereby intense SACZ events are modulated by the MJO (Carvalho *et al.*, 2004). Composite analysis performed by Liebmann *et al.* (2004) supports these findings, revealing statistically significant variations in precipitation both downstream of the South American low-level jet (SALLJ) and within the SACZ depending on the phase of the oscillation. The MJO activity was found to be influential in enhancing upper level cyclonic and low-level anticyclonic anomalies, which are both features of a strengthened SALLJ.

Shimizu *et al.* (2017) explored the relationship between extreme precipitation events in the Amazon basin and phases of the MJO and ENSO activity. Extreme wet events in the Amazon were found to be more frequent when the MJO was active, particularly when tropical convection was strongest over the Indian Ocean (phases 1 and 2) and during phases 7 and 8 when convective activity is reduced over Australia. Shimizu *et al.* (2017) also note that despite the frequency of wet events being at its highest during phase 7 of the MJO cycle, considering cases for only the MJO events (i.e. not accounting for the ENSO), precipitation and convective motion were strongest in phase 2, indicating that events may become more extreme when the MJO is positioned over the Indian Ocean.

4.1.4 | Pacific decadal and Atlantic multidecadal oscillations

Studies analysing the impact of the PDO and AMO on rainfall variability tend to explore the relationship indirectly, focusing on how the PDO/AMO phases modulate the ENSO characteristics (e.g. Wang *et al.*, 2014; García-García and Ummenhofer, 2015). For instance, the frequency and intensity of the ENSO anomalies have been found to be controlled by the phase of the PDO, with an intensification of wet/dry anomalies identified when the ENSO and PDO are in phase (e.g. a warm PDO and El Niño; Wang *et al.*, 2014). Moreover, when the ENSO and PDO are out of

phase, typical the ENSO and climate relationships were found to weaken or even disappear. For instance, during the cold phase of the PDO, precipitation anomalies associated with El Niño conditions are weakened over northern South America, including within parts of the Brazilian Amazon basin (Wang *et al*., 2014). These results were previously identified by Kayano and Andreoli (2007) who concluded that the strength of the ENSO teleconnections is potentially related to the phase of the PDO, with composites of rainfall for El Niño and La Niña years over South America substantially different between the PDO phases.

For the AMO, an opposing relationship emerges, with cold (warm) AMO regimes associated with stronger (weaker) ENSO variability (Timmermann *et al*., 2007; García-García and Ummenhofer, 2015). In other words, the ENSO events, in general, tend to be stronger when the two indices of the SSTs are out of phase (e.g. El Niño and a cold AMO regime), with the positive AMO regime characterised by anomalous easterly winds over the central and western Pacific that deepen the thermocline in the west Pacific (García-García and Ummenhofer, 2015). Over South America, anomalous precipitation composites showed more (less) organised patterns of rainfall, with significant anomalies occupying more (less) land area when the ENSO and AMO are in the opposite (same) phase (Kayano and Capistrano, 2013). Direct studies between the AMO and Amazon rainfall have shown positive phases of the AMO are linked to increased drought frequency (Barichivich *et al*., 2018) and the shortage of rainfall during the 2005 and 2010 mega-droughts (Aragão *et al*., 2018). A recent study by Kayano *et al*. (2019) explored the concomitant influence of the AMO and PDO phases on La Niña teleconnections over South America. The highest (lowest) number of La Niña events occurred during periods in which warm AMO/cold PDO (cold AMO/warm PDO) persisted, consistent with what is expected based on the previous literature (e.g. Kayano and Capistrano, 2013; Wang *et al*., 2014; García-García and Ummenhofer, 2015). Considering other backgrounds, a combination of a cold AMO/cold PDO represented a larger percentage of La Niña events relative to a warm AMO/warm PDO, suggesting the importance of the cold PDO phase in favouring La Niña SST anomalies in the Equatorial Pacific.

4.2 | River discharge variability

4.2.1 | Pacific influence

Marengo et al. (1993) identified using observations and simulations that the variability of river flows in the Amazon can differ on the order of two standard deviations between El Niño and non-El Niño years. More recently, Emerton *et al*. (2017) produced historical probabilities of the chances of observing abnormally high or low streamflow for the entire globe in response to El Niño and La Niña events for both the year in which an event peaks and for when it decays. For the Amazon, regions south of the Amazon River, particularly towards the western side of the basin are likely to observe higher than usual river flows during August and September for El Niño years during the initial stages of an ENSO event (40–60% probability) (Figure 4c). The signal reverses in the Brazilian Amazon for months closer to boreal winter, when El Niño typically reaches its peak. From November, lower than usual flows dominate the Brazilian Amazon with the signal strongest during December and between May and July during the decaying phase (Figure 4b,c). Drier conditions are dominant in the northeastern Amazon throughout both the wet and dry seasons, which occur slightly later than those noted for rainfall due to the large lag between rainfall and discharge peaks (Figure 4b,c).

For La Niña years (i.e. the cold phase of the ENSO), the signal is generally weaker across the basin. Towards the northwest, around the confluence point of the Solimões River, where the headwaters of the Marañón and Ucayali rivers meet and in the western Brazilian Amazon, drier-than-usual flows are more likely in September and December (Figure 4f). In contrast, increased river flows are more likely in the northeastern Amazon above the Amazon River from as early as July and lasting until around the following July. This signal is strongest during February and March as La Niña begins to decay and extends into the southern Amazon during December (Figure 4e,f).

Analysis using observed river discharge data have identified similar signals for mean annual river flows, with lower (higher) levels of discharge during El Niño (La Niña) years found in all river basins with the exception of the southern Madeira basin (Espinoza *et al*., 2009a), consistent with results of Ronchail *et al*. (2005b) (Figure 4a,d). Major negative anomalies during El Niño are observed in tributaries in the northeastern Amazon, similar to the response for rainfall (Figure 2a) and at Altamira station, located downstream of the southern Xingu River (Figure 4a) (Ronchail *et al*., 2005b). The signal in the north is replicated in several further studies (e.g. Uvo and Graham, 1998; Foley *et al*., 2002; Schöngart and Junk, 2007) with improved skill at forecasting discharge in northern sub-basins when using the Pacific SSTs (Uvo and Graham, 1998; Uvo *et al*., 2000). River flows in the Negro River were found to be significantly lower during El Niño years relative neutral conditions, whilst the opposite is true for La Niña (Figure 4b,e) (Schöngart and Junk, 2007).

Other notable regions include tributaries positioned to the east of the Madeira River (Ji-Parana, Aripuana,

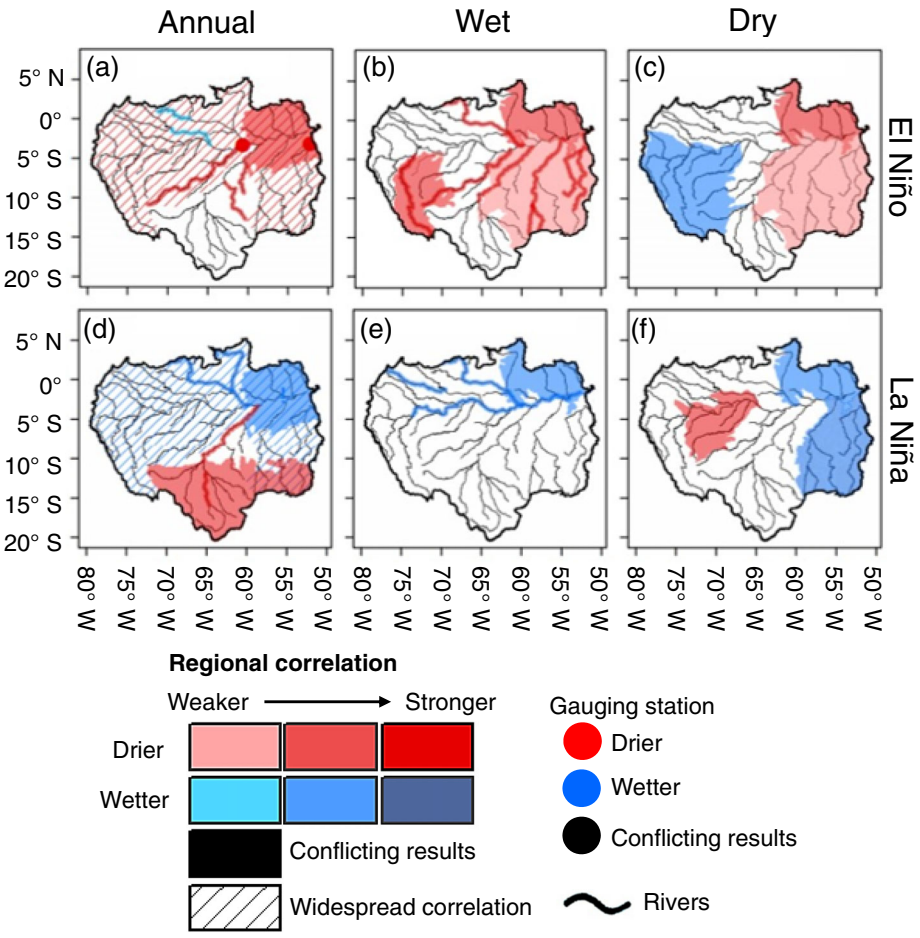

FIGURE 4 Influence of El Niño Southern Oscillation (ENSO) conditions on river discharge in the Amazon basin based on results identified within the literature: (a, d) the entire year; (b, e) the Amazon wet season (February–June); and (c, f) the Amazon dry season (August–December). The legend is the same as for Figure 2. For full details of the reference(s), type of analysis used and strength of the relationships, see Tables S19–S24 in the additional supporting information

and Sucunduri), which witness up to a 25% decrease in discharge during El Niño phases (Ronchail *et al.*, 2005b). An opposing signal (i.e. higher than normal river flow) was evident in the Japura River towards the Colombian Amazon and in the upper Negro basin (Figure 4a). Positive anomalies during La Niña events are predominately observed towards the northeastern Amazon and along the Branco River, with lower than usual river flows more common in southern tributaries, particularly in the Mamoré and Madeira rivers (Figure 4d).

These studies support the global analysis of Ward *et al.* (2010), who investigate the sensitivity of annual mean, one and seven day maximum river discharge to the ENSO. They observed a positive relationship (i.e. drier conditions during El Niño) at all stations within the tropics, associated with the anomalous displacement of the Walker circulation. No statistical differences were found in the sensitivity to the Southern Oscillation Index (SOI) between mean and maximum discharges. This means the impacts of the ENSO were not found to be stronger for high flows compared with mean conditions, as is observed in many areas of the world.

4.2.2 | Atlantic influence

Espinoza *et al.* (2009a) find that for the TNA discharge variability in Amazonian rivers responds similarly to the ENSO. A negative correlation is identified between the TNA SSTs and mean and annual maximum river flows, indicating that when the TNA is warmer than usual, river discharge decreases (Figure 5a), highlighting the same response to rainfall (i.e. a decrease in rainfall). This similar response to both the ENSO and TNA SSTs can be explained by positive correlations between the two indices. Several studies have highlighted the impact of the ENSO on the tropical Atlantic SSTs (Enfield and Mayer, 1997; García-Serrano *et al.*, 2017) and its reversal through the induction of low-level cyclonic atmospheric flow due to the warming of TNA SSTs in boreal spring (Ham *et al.*, 2013).

This relationship for lower than usual river flows was observed in most sub-basins except for the southern Madeira and northern Branco rivers, with the colder than usual TNA SSTs found to produce the opposite effect (Espinoza *et al.*, 2009a) (Figure 5b). Marengo (1992) identified when the anomalously cold SSTs in the TNA occur concurrently with a warmer than usual TSA, water levels

in the Negro River are generally higher (Figure 5b,c). These results are consistent with those produced by Ronchail *et al.* (2005b) for most regions of the Amazon. Stations situated between the Amazon River and 10° S showed higher than usual low and mean flows when the TNA is colder than usual, though an inverse relationship was observed in the Branco River basin in the far north (Figure 5b).

Considering the TSA, identified as being less important for Amazon rainfall (Yoon and Zeng, 2010), the relationship with discharge is more complex and is considered time dependent (Ronchail *et al.*, 2005b). For instance, between 1974 and 1994, a warm TSA was linked with higher river flow in the Beni River basin (Figure 5c). In contrast, the Mamoré-Madeira basin, located just east of the Beni and Madeira rivers, increased discharges that corresponded to anomalously cold conditions (1988–2001) (Figure 5d). This relationship in the southern Amazon highlights the problems that could arise when using SST anomalies for potential flood prediction, with wetter conditions found in neighbouring sub-basins for opposing SST anomalies.

4.2.3 | Other drivers

There is an absence of literature focusing on the influence of the MJO, PDO and AMO on river flows in the Amazon basin relative to indices on shorter timescales (e.g. the ENSO). For several indices of longer term Atlantic and Pacific variability, only the AMO and the cross-equatorial Atlantic SST (Deser *et al.*, 2010) indices were significantly and negatively correlated with variations in minimum dry season water levels at Manaus gauging site (Barichivich *et al.*, 2018). Lee *et al.* (2018) observe the same negative correlation with seasonal peak flows in central South America providing "fair" predictions of seasonal flows based on a global scale prediction model evaluated using the categorical Gerrity skill score (GSS). These results are consistent with the typical relationship found between rainfall, river discharge and warmer conditions in the north Atlantic, with drier conditions dominating throughout much of the Amazon owing to the northward displacement of the ITCZ. This highlights the dominant role of the tropical Atlantic in modulating drought frequency in the Amazon and thus the ability to predict periods of dry spells.

The modulation of flooding or periods of abnormally high flows at longer timescales is much less understood (Barichivich *et al.*, 2018). Recent studies have shown some predictability with regards to the strengthening of the Walker Circulation and associated enhancement of the Equatorial trade winds in the Pacific Ocean, which may offer multiyear predictability in some parts of the world (McGregor *et al.*, 2014; Espinoza *et al.*, 2016). In the Amazon, variations in maximum water levels at Manaus gauging station are consistently correlated with the strength of the Pacific trade winds (averaged 10 m zonal winds; Barichivich *et al.*, 2018) and the SST gradients between the Atlantic and Pacific oceans basins (Chikamoto *et al.*, 2015). The mechanisms behind this strengthening can be related to the dynamics of trans-basin variability (TBV), which is defined as the difference between the area-averaged Atlantic and Pacific SSTs. McGregor *et al.* (2014) implemented a basin-scale TBV index, defined as the monthly mean difference of the Atlantic–Pacific SST anomalies. They show how the TBV index is heavily influenced by the strength of the trade winds and operates on a frequency of roughly five years. Around 1991, cool Atlantic conditions featured alongside a relatively warm eastern Pacific, resulting in a negative TBV phase where Pacific trade winds were anomalously weaker. Since the late 1990s, rapid warming in the Atlantic Ocean (Gloor *et al.*, 2013) combined with subsequent cooling in the eastern Pacific led to a reversal in the TBV index, whereby the Equatorial trade winds were enhanced due to anomalous low (high) pressure over the Atlantic (Pacific) oceans. This enhancement is found to coincide with a 55% increase in wet-day frequency ($> 10\ mm{\cdot}day^{-1}$) in the western Amazon (Espinoza *et al.*, 2016).

Indices that operate at lower frequencies (e.g. the TBV, PDO and AMO) could translate into useful information for the risk assessment for various sectors operating in the Amazon (e.g. agriculture). However, unlike for the relationship between droughts and warmer than usual North Atlantic SSTs, the mechanisms behind flooding at longer timescales still require further research.

4.3 | Rainfall versus river discharge

Overall a similar relationship is clear between the phases of the ENSO and the trends seen in both rainfall and river discharge, particularly on annual timescales (Figures 2 and 4). During El Niño events, drier conditions are prevalent, while increased rainfall and river discharge are generally found throughout the basin during La Niña. Changes in association to the ENSO are strongest in the northeastern Amazon for both variables. Some discrepancies appear during the dry season for La Niña years, with less rainfall noted in the southern Amazon (Figure 2f), while a reduction of discharge is only observed in parts of the northwestern Amazon (Figure 4f). It should be noted that the dry season typically overlaps when ENSO is in its initial building or decaying phase, with a stronger association generally acknowledged during

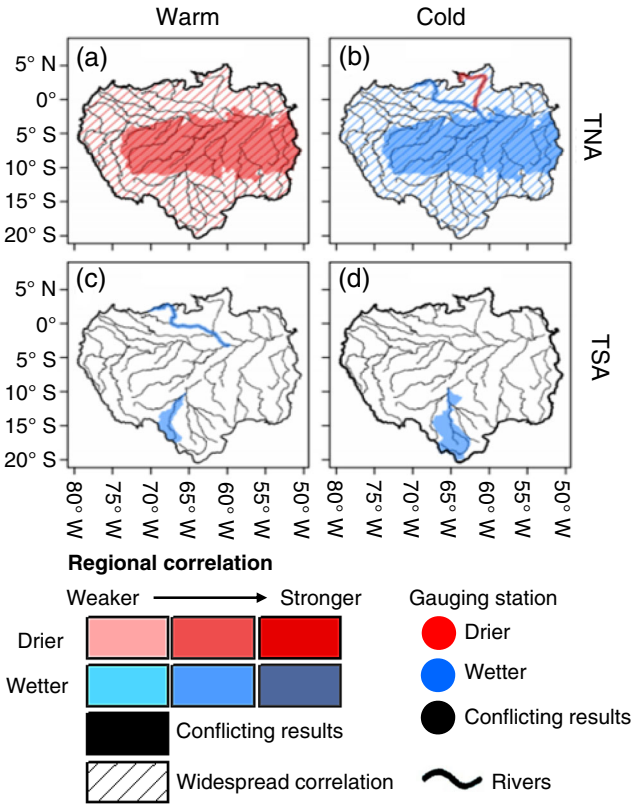

FIGURE 5 Influence of tropical Atlantic sea surface temperatures (SSTs) on river discharge in the Amazon basin based on results identified within the literature: (a) a warm Tropical North Atlantic (TNA), (b) a cold TNA, (c) a warm Tropical South Atlantic (TSA) and (d) a cold TSA. Results are only shown for the entire year owing to the limited number of studies that have seasonal results. The legend is the same as for Figure 2. For full details of the reference(s), type of analysis used and strength of the relationships, see Tables S25–S28 in the additional supporting information

December–February when the ENSO reaches its peak. For the Atlantic, rainfall and discharge respond similarly, with a reduction in rainfall and discharge when the TNA is anomalously warm and an increase when the TNA is colder than usual. The TSA is found to be less influential for both variables (Figures 3 and 5).

In addition to magnitude, the SST variability has been shown to affect the onset and withdrawal timings of the wet season. In the central Amazon, the average onset date was determined to be around September 25 when constructing five day rainfall averages (pentads), and is associated with anomalous anticyclone activity and enhanced trade winds in the Atlantic (Marengo *et al.*, 2001). The combination of the cold Atlantic and warm Pacific SST anomalies is linked with a delayed onset and early withdrawal of wet season rainfall. For this particular configuration of the SSTs, there is an observed delay in the seasonal migration of peak convection from the Northern to the Southern hemisphere, owing to the delay of planetary boundary layer (PBL) moisture. This build up of the PBL moisture is responsible for the onset of convection, with regions closer to the Equator more sensitive to small changes in the thermodynamic and dynamical structure of the atmosphere relative to the southern Amazon (Fu *et al.*, 1999). Thus, central and northern catchments are likely to be more sensitive to changes in the SSTs in the adjacent oceans.

So far, the aforementioned studies have described the role of the tropical Atlantic and Pacific oceans in determining precipitation variability in the Amazon basin. However, Builes-Jaramillo *et al.* (2018) hypothesise that the interaction between the SSTs in the Atlantic and the hydrology of the Amazon are more complex, proposing a two-way feedback system. They identify that shifts in the hydrology of the Amazon can influence future states of the TNA SSTs up to two months in advance. When the Amazon is particularly dry (wet), atmospheric surface pressure over the Amazon increases (decreases). Consequently, the atmospheric surface pressure between the TNA and the Amazon is reduced (increased), which in turn reduces (enhances) the zonal trade winds. As the zonal trade winds weaken (strengthen) over the TNA, there is reduced (increased) evaporative cooling leading to an increase (decrease) in the TNA SSTs.

It is important to highlight the fact that the majority of correlations described in Section 4 are often considered for larger catchment areas and/or for a small number of meteorological/hydrological stations. This is particularly true for precipitation in smaller sub-basins, which suffers from poor spatial coverage (Paccini *et al.*, 2018). Consequently, the relationship between rainfall and climate drivers can be difficult to assess.

5 | HYDROCLIMATIC DRIVERS AND EXTREME FLOOD EVENTS

Figure 6 shows all the flood events outlined in Table 2 plotted onto the times series of the SST anomalies for the El Niño 3.4, TSA and TNA regions. It should be noted that these floods were based on what was identified within the literature and flood databases, and so it is biased towards regions where more research and flood recordings take place. The southwestern Amazon, for example, shows more floods through time, but this could be due to flood events being recorded and analysed more frequently in these locations. In addition, southwestern regions have several gauging stations where floods tend to be analysed (d–i), whereas floods in the Peruvian Amazon are generally based on water levels at Tamshiyacu

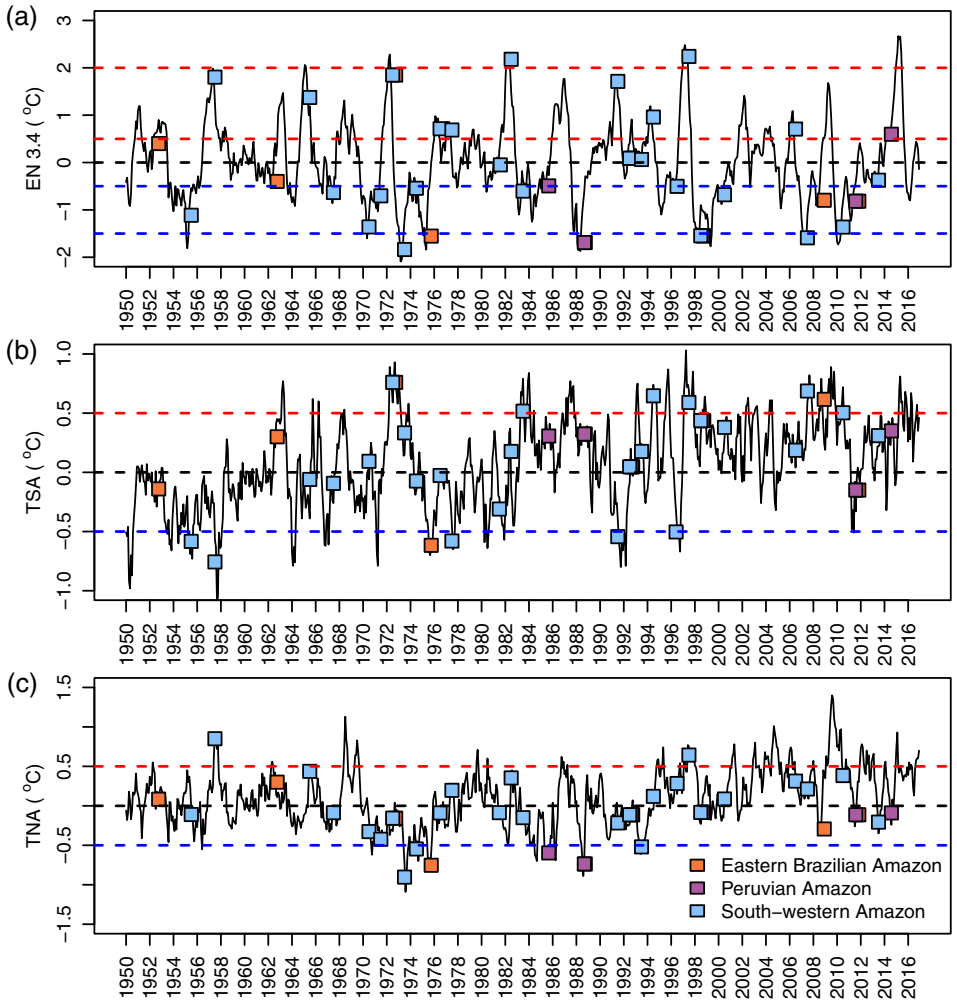

FIGURE 6 Amazon flood events from Table 2 plotted onto the time series of the sea surface temperature (SST) anomalies in the tropical Pacific and Atlantic oceans: (a) El Niño 3.4 region, (b) Tropical South Atlantic (TSA) and (c) Tropical North Atlantic (TNA). Floods are based on the gauging stations that match those shown in Table 2, with colours representing the region in which the flood occurred. Circles are positioned during the month of occurrence (i.e. *x*-axis) with the height (i.e. *y*-axis) determined by the preceding October–December (March–May) mean SST anomaly for the El Niño 3.4 (TNA and TSA) regions. Dashed blue and red lines depict the threshold for the respected warm and cold phases of each index (e.g. –0.50°C for a weak La Niña event and 2.0°C for a very strong El Niño, as classified for the Oceanic Niño Index (ONI)

gauging station (a). Figure 6 also highlights that flood events can occur in several regions of the basin regardless of whether the SST anomalies are in their positive, neutral or negative phases. This implies that although flooding in a certain location may be linked to a particular phase of climate (e.g. La Niña), floods are not restricted to this particular phase and demonstrates the complexities that exist when making any association with a particular hydroclimatic driver.

5.1 | Attribution of drivers

5.1.1 | Lower confidence attribution case: The 1993 Peruvian Amazon event

Indices of hydroclimate drivers are of interest for flood forecasters and humanitarian organisations alike due to the potential for their use in increasing the predictability of upcoming floods. However, in some cases, the links between floods and hydroclimate drivers are not clear. Figure 6 plots each flood event identified in Table 2 over the time series of the SST anomalies in the tropical Pacific and Atlantic oceans. Some floods, such as those observed at Tamshiyacu (a), in 1993, have previously been associated with La Niña conditions during the preceding austral spring and summer (Espinoza *et al*., 2013). Considering the region (5° N–5° S, 120–170° W), the SST anomalies in the central Pacific in the build up to this event did not in fact reach the typical ONI −0.5°C threshold (weak La Niña) for any three month period (preceding October–December mean = −0.28°C) (Figure 6a), with the positive SST anomalies observed from January 1993 onwards. Similarly, the 1986 event, also attributed to La Niña conditions (Espinoza *et al*., 2013), never broke the −0.5°C threshold during austral spring and summer, though the negative SST anomalies were persistent throughout the period. This means it is unlikely that these floods were due to La Niña conditions and that a different response mechanism could be responsible.

Analysis for these events was centred around a composite of the SSTs, geopotential height and vertical integrated humidity flux anomalies for the four strongest flood years at Tamshiyacu gauging site (a) (1993, 1986,

1999 and 2012) for the preceding October–December season (Espinoza *et al*., 2013). Atmospheric anomalies were identified and found to be responsible for increased moisture convergence over the northwestern Amazon. This analysis was performed for the mean of the four years, which included the stronger La Niña conditions observed in austral summer during 1998 and 2011, with the atmospheric response to individual events only mentioned for 2012. It is therefore currently unknown if the oceanic conditions in the Pacific in the build up to the 1993, 1986 and 1999 floods were capable of reproducing the same or a similar atmospheric response that could be determined as the cause for those events. Further investigation of the SST anomalies and atmospheric response to each individual event (as performed for the 2012 flood) rather than as a composite could form a useful task in identifying the relationship between the magnitude and location of cooling in the central equatorial Pacific and the level of humidity flux convergence over the Amazon basin. Such an analysis could allow more confidence in the understanding of the magnitude of the SSTs required to favour an atmospheric response that commonly produces severe flooding.

Other cases also exist, for instance, for the 1953 floods at Óbidos (b), Brazil (Table 2). Here, the link to climate is often not directly stated (e.g. Marengo and Espinoza, 2016) (Table 1), whereas in other works (Marengo *et al*., 2013a) (see Section 2) it has been connected to a warmer than usual TSA in the absence of La Niña. Though, as shown in Table 2 and Figure 6b, the SST anomalies in the TSA are mostly negative throughout the entire preceding year to the event with a minimum temperature anomaly of −0.29 in April 1953.

5.1.2 | Higher confidence attribution case: The 2014 Brazilian Amazon event

The 2014 extreme floods affected many locations within the southwestern Amazon, particularly in the Madeira basin with river discharge reaching a record breaking 58,000 $m^3 \cdot s^{-1}$ at Porto Velho gauging station (e) (Table 2). Espinoza *et al*. (2014) first identified anomalies in hydrological conditions, with higher than normal rainfall observed as early as September 2013, peaking towards the end of January 2014. Examining large-climatological features in the build up to the event (i.e. the wet season from December to March), a negative TSA–SSA gradient was attributed to the event with the exceptionally warm SSTs in the SSA present from January 2014.

These conditions were associated with a change in atmospheric circulation from January to March 2014. Positive 850 hPa geopotential height anomalies were found to produce anomalous anticyclonic circulation, which extended from the SSA into South America and was responsible for a weakening of the SACZ activity and an enhancement of the SALLJ bringing anomalous rainfall. Moreover, vertically integrated vapour transport anomaly fields from December 2013 to March 2014 showed an intense incursion from the TNA to the southern Amazon (Espinoza *et al*., 2014).

Further analysis involved using a composite analysis to investigate floods in the region which were not associated with La Niña. As in Espinoza *et al*. (2013), the climatological conditions were averaged for four flood years (1978, 1982, 2001 and 2014), producing an TSA–SSA SST gradient and a positive 850 hPa in the SSA region. However, humidity composites were then compared with those solely for the 2014 event and revealed that the incursion of the humidity flux from the tropical Atlantic was more intense for this specific event.

As climatological conditions (i.e. the SST anomalies, geopotential height anomalies and humidity fluxes) were analysed solely for conditions witnessed in the build up to the 2014 event (i.e. December 2013—March 2014), greater confidence can be obtained in the attribution of the flood compared with years in which conditions were only presented for averaged conditions (i.e. 1978, 1982 and 2001). This is the same case for the 2012 Peruvian Amazon flood (Espinoza *et al*., 2013), whereby a single flood year is analysed in addition to a composite of years. It is important to recognise that this does not imply that the other flood events within the composite are not associated with atmospheric circulation patterns sourced from a strengthened TSA–SSA gradient, but rather the specific climatological response for each individual event is less known. Further numerical modelling analysis investigating the ocean–atmosphere mechanisms behind flooding is still required. Comparisons between conditions of similar events may help explain differences in intensity and persistence (Espinoza *et al*., 2014), and provide useful information to provide early warnings for future floods.

5.2 | Classification of a flood

Most of the large Amazonian rivers experience a single flood period with overbank flow in a "normal" year. This is why, when reviewing the literature, discrepancies appear in the classification of a flood event. Should a flood be classified based on a threshold of streamflow exceedance, the number of days above threshold, the extent of inundation, by riverbank exceedance or by socioeconomic impact? In the introduction to Vauchel *et al*. (2017), a discharge > 6,000 $m^3 \cdot s^{-1}$ at Rurrenbaque gauging station (d) (Beni River) is determined as a flood

event based on the average high flood level when evaluating floods against the ENSO frequency. However, this level is exceeded almost every year, making any association with the ENSO phases difficult.

Another example includes the 250,000 $m^3 \cdot s^{-1}$ discharge threshold used by some authors (e.g. Callède *et al*., 2004; Ronchail *et al*., 2006) at Óbidos (b). Though this value represents the water level at which the town begins to inundate (Callède *et al*., 2004), streamflow observations for this station show this level is regularly exceeded, despite no significant impacts or reports of extreme flooding being registered every time (e.g. between May and July 2010). Thus, thresholds used for decision-making, flood warnings and forecasting research could be better chosen to reflect the risk to communities in a particular reach of a river as opposed to a magnitude of river flow that causes a river to exceed its banks.

5.3 | "Normal" versus "extreme" floods

It is also important to understand how a "normal" flood is distinguished from an "extreme" flood. A case is presented in the upper Madeira basin, where in 2007 and 2008 rainfall was higher than the climatological average producing flooding along the Mamoré (g) and Guaporé rivers (Table 2). Ovando *et al*. (2016) state that in terms of river discharge, the floods would be better classified as "above normal", but argue they should be considered "extreme" due to their socioeconomic impact. The two floods combined reportedly affected > 250,000 people, resulting in 49 fatalities (CEPAL, 2008).

For better classification, both flood hazard and flood risk should be considered. For instance, when assessing how climate variability affects flood hazard, it is important to use measures of flooding that are hazard related (e.g. streamflow, water level and flood extent). Whereas for the EWS and humanitarian protocols (e.g. FbF; Coughlan de Perez *et al*., 2015) it is the flood risk that becomes more important; thus, statistics and information including economic cost, the number of people exposed or implications for local populations (e.g. food provisions) are a more suited measure of flood severity. It is therefore necessary to recognise both, as in Langill and Abizaid (2019), as a flood-type analysis for a village located along the Ucayali River in Peru. In their analysis, the authors used a combination of hydrograph (i.e. water level, high-water period and onset dates) and field data (i.e. interviews with community members) to help distinguish what makes a "bad" or "extreme" flood. Four flood types (high, long, early and late) are classified, the authors concluding that while high floods are the most common, long and early floods occur on a similar frequency and tend to have more severe implications for people.

5.4 | Flood mechanisms during La Niña

Figure 7 displays a schematic of the step-by-step processes in which the abnormal SST conditions can drive atmospheric behaviour and consequently cause excessive rainfall and flooding in the northwestern Amazon. It is important to highlight that the mechanisms behind flood events often differ depending on the exact location within the basin (e.g. upstream in the northwest versus downstream in the Brazilian Amazon; Espinoza *et al*., 2013). These processes have been determined by the occurrences of events in the build up to previous floods from studies in the literature:

- During typical conditions, the equatorial trade winds blow east to west (i.e. easterly trade winds). Consequently, warmer surface waters in the central Pacific are pushed west towards Indonesia, raising the water levels in the region relative to those found off the coast of Peru. To compensate, deep colder waters rise off the coast of Peru (i.e. cold-water upwelling) in order to replace the warmer waters that have been transported by the surface winds. During La Niña, the easterly trade winds that carry large quantities of moisture are enhanced (Figure 7a) owing to decreases in pressure in the Indonesian continent relative to the central and eastern Pacific.
- This results in warmer surface waters in the central Pacific being pushed further west, increasing the upwelling of cold water and causing cooler than usual SSTs in the central to eastern Pacific. The ENSO events typically reach their peak during the boreal winter (Emerton *et al*., 2017), with previous Amazon floods associated with colder than usual SSTs from October–December onwards (Espinoza *et al*., 2013). During La Niña, the negative SST anomalies dominate the central equatorial Pacific, usually on the order of −1 and −2°C during strong events. The positive SST anomalies are often observed over the northern and southern Pacific and Atlantic oceans (either side of the negative anomalies), whilst cooler than usual waters are found off the coast of Brazil in the Atlantic Ocean (about 20° S) (Satyamurty *et al*., 2013).
- This pattern of the SSTs favours positive 850 hPa geopotential height anomalies over both the northern and southern Pacific and Atlantic oceans, with the stronger positive SSTs in the northern and southern Pacific resulting in stronger positive 850 hPa geopotential height anomalies (Espinoza *et al*., 2013) (Figure 7b). Negative 850 hPa anomalies are also observed between the positive anomalies (about 125° W).

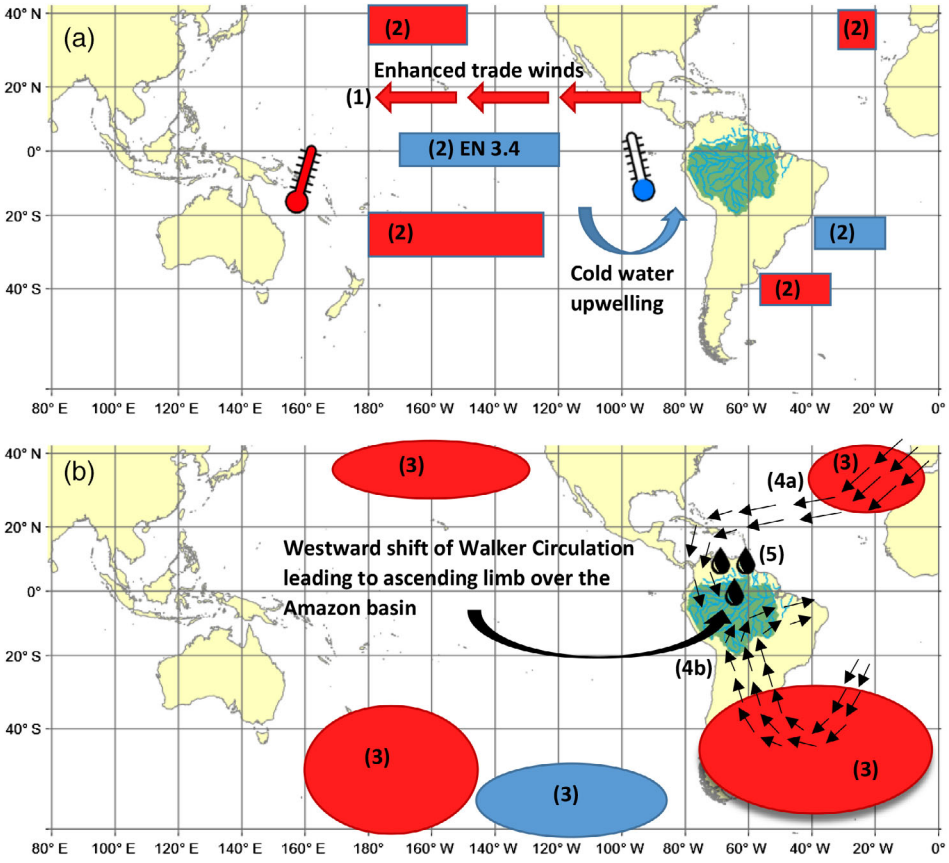

FIGURE 7 Step-by-step climatic features associated with floods attributed to La Niña: (a) enhanced trade winds, cold water upwelling and sea surface temperature (SST) anomalies; and (b) 850 hPa geopotential height anomalies and humidity transport fluxes. Red (blue) colours represent positive (negative) anomalies of the SST and 850 hPa geopotential height; circles represent geopotential heights anomalies; squares/rectangles denote SST anomalies; and numbers refer to the specific processes explained in Section 5.4

- The succession of positive and negative 850 hPa geopotential height anomalies, features a Rossby wave response from October to December, in which warm air is transported from the Equator towards the Poles in an attempt to restore the atmospheric energy balance. These geopotential height patterns are shown to favour the enhancement of moisture convergence towards the Amazon basin *via* two mechanisms (Espinoza *et al*., 2013):
- The easterly humidity flux is intensified over the North Atlantic and is directed towards the Caribbean Sea by the positive geopotential height anomaly situated in the North Atlantic before moving southwards towards the northwestern Amazon (Figure 7b).
- The southward positive geopotential height anomaly in the Atlantic is responsible for generating humidity fluxes that progress northwards near the Andes, reducing the monsoon flux towards the La Plata basin and the strength of the SLLJ which is responsible for transporting large amounts of moisture from the Amazon basin to the subtropics (Montini *et al*., 2019), and thus helping to maintain higher levels of humidity over the Amazon basin.
- In addition to these two humidity fluxes, the SST pattern associated with La Niña results in the Walker Circulation shifting farther west, whereby the ascending limbs of moist air are situated over both the maritime continent and South America resulting in positive rainfall anomalies (Yeh *et al*., 2018).

Owing to the mechanisms described by Espinoza *et al*. (2013) for moisture convergence, it seems the intensity and locations of the 850 hPa geopotential height anomalies are pivotal to create the required atmospheric circulation for maintaining the convergence of humidity fluxes over the Amazon basin. As mentioned, these geopotential height anomalies are positioned where warmer than usual SSTs are situated in the northern and southern Pacific and Atlantic oceans and are stronger as the SSTs increase. Therefore, though the typical ENSO 3.4 region in the central Pacific is often used as the index to predict flooding through its role in shifting the Walker Circulation, these others zones of the SST variability could be influential in the prediction of upcoming events and deserve further investigation.

6 | CONCLUSIONS

This review discusses out what is currently known about how climate variability influences rainfall, river discharge and flooding in the Amazon basin. This information is a

key component in aiding flood prediction, providing potential sources of predictability at interannual to decadal timescales to enable the possible implementation of early warning systems (EWS). Based on evidence from studies in the published literature, it is clear that dry spells in the Amazon are driven by the warm phase of the El Niño Southern Oscillation (ENSO) and warmer than usual sea surface temperatures (SSTs) in the Tropical North Atlantic (TNA), particularly affecting the southern Amazon. While wetter conditions and flooding are often associated with the cold phase of the ENSO and to a combination of warm (cold) SST anomalies in the Tropical South Atlantic (TSA) (TNA). However, the meteorological and hydrological response in association with climate patterns such as La Niña are still not fully understood, and evidence for their usefulness for flood forecasting remains weak. Though there is a clear link between hydrometeorological variables and certain phases of climate, more research is required in calculating the probabilities of flood risk during certain climate patterns, particularly for years in which multiple climate variations feature simultaneously (e.g. a warm TSA and La Niña), and then communicating this information in an informative way to aid decision-making. Here, we identify five areas in which to focus research efforts to better understand how climate variability impacts flood risk in the Amazon basin.

6.1 | Uncertainties and lack of evidence

The relationship between climate indices and hydrometeorological variables (i.e. rainfall and river discharge) can be highly uncertain owing to a range of factors. First, though strong correlations do exist between the ENSO and hydrometeorological variables, no two ENSO events are exactly alike (e.g. different temporal evolutions, spatial and magnitude differences of the SST anomalies), with asymmetrical differences found between the cold and warm phases (Cai *et al*., 2020). This is highlighted by several authors (Hill *et al*., 2009, 2011; Rodrigues and McPhaden, 2014) who have identified different or even opposing rainfall anomalies in different regions of the world depending on whether the centre of cooling or warming in the equatorial Pacific Ocean was central or eastern specific. Such differences are associated with the location of the SST anomalies modifying the Walker Circulation and, hence, upward convection and rainfall locations (Hill *et al*., 2009). Further evidence is required to understand the hydrological response in basins to the diversity of possible climatic events.

The back-water effect (Meade *et al*., 1991) and autocorrelation could also have an impact on correlations between climate phases and river flow as some commonly used statistical tests (e.g. Mann–Kendall and linear regression) may not be suitable for certain regions and rivers that have a large-basin memory (Marengo *et al*., 1998). Where autocorrelation exists, correlations may be overestimated and identify significant relationships where they do not exist, consequently leading to misleading significance. It is therefore an important reminder to consider running suitability checks on data before any climate analysis is undertaken. Such checks include plotting river flow using a correlogram (i.e. correlation of series data with itself), running a Durbin–Watson test and checking for trends and correlations for both rainfall and river discharge where possible owing to autocorrelation issues being less likely in rainfall data (Marengo *et al*., 1998).

The robustness in changes to hydrological variables are also debatable due to the observational records in both hydroclimatic drivers (e.g. the ENSO) and individual hydrological time series being limited in time (Wittenberg, 2009; Marengo and Espinoza, 2016; Marengo *et al*., 2018; Yeh *et al*., 2018). For instance, in the southern Amazon, the effect of the anomalous SSTs in the Atlantic Ocean on river discharge is dependent on the time period investigated, with an opposing response to the SST anomalies identified in neighbouring basins (Ronchail *et al*., 2005b). In this and similar works, the period of investigation is often limited to between 10 and 20 years, where few climate events (e.g. El Niño) feature, preventing strong conclusions to be made. This is particularly problematic when considering the relationship for lower frequency climatic drivers (e.g. the PDO and AMO) that operate on decadal to multi-decadal timescales, as many station time series may only exist during one particular phase. Newly developed climate reanalysis and hydrological models can produce data sets that can extend the analysis back to 1950 (e.g. ERA-5; Zsoter *et al*., 2019), though the accuracy of simulated streamflow data requires robust evaluation. A model run incorporating ERA-5 as the meteorological input into a hydrological model was found to improve the ability to simulate annual peak river flows in the Amazon basin, particularly at stations situated within the Peruvian Amazon (Towner *et al*., 2019). The ERA-5 is now fully accessible back to 1950, and with the release of ERA-5 land, which incorporates the evolution of land surface variables (e.g. soil temperature) over several decades at an enhanced resolution compared with ERA-5 (ECMWF, 2020), and thus further investigation is required.

6.2 | Understanding flood mechanisms

To enhance the predictability of flooding in the Amazon basin, more focus is needed to understand the

mechanisms behind individual events and their potential to provide predictability. Two of the most extreme flood events (2012 in Iquitos and 2014 in the Madeira basin) were assessed individually (Espinoza *et al*., 2013, 2014), highlighting the mechanisms and atmospheric response associated behind each flood event in response to climate anomalies present in the atmosphere and surrounding oceans. However, other devastating, but less extreme, floods such as those observed in 1989, 1993 and 1999 are currently restricted to composite analysis in which the climatic conditions are smoothed across multiple events. Although the average conditions have been shown to produce atmospheric conditions responsible for flooding (e.g. Espinoza *et al*., 2013), it is unknown if the climate anomalies, which are weaker for certain events, would result in the same atmospheric response. Numerical analysis and modelling of the ocean–atmospheric response to each event individually could allow further evidence to be obtained in understanding the characteristics of the SST anomalies required to produce flooding across the basin (e.g. the spatial distribution and magnitude of the SSTs). Although complicated by the non-linearity in the response to climate phases such as the ENSO (Frauen *et al*., 2014) and by the limited number of observed events, such an analysis could provide useful information to flood forecasters and decision-makers within humanitarian sectors.

6.3 | Flood timing and additional indices

In March 2018, the Red Cross led an inter-agency assessment mission to assess how communities in the Peruvian Amazon were affected during particularly strong flood events, such as those observed in 2012 and 2015 to aid decision-making. Problems associated with the duration of the wet season rather than solely the magnitude of extreme flooding was highlighted by residents living within the floodplain (Bazo, 2018). Several authors (Ronchail *et al*., 2006; Tomasella *et al*., 2011; Marengo *et al*., 2012; Espinoza *et al*., 2013; Langill and Abizaid, 2019) highlight the importance of flood timing in major Amazonian tributaries in the dampening or superposition of the travelling Amazon flood wave along the main stem. Therefore, we encourage more authors to consider both flood timing and duration in addition to flood magnitude when investigating the influence of different phases of large-scale climate variability. In addition, many studies focus on the conventional SST and sea-surface pressure definitions of the ENSO events, disregarding atmospheric variables such as outgoing long wave radiation (OLR) and zonal wind speeds, which have been proven to show to improved predictability in certain regions of the world (Chiodi and Harrison, 2013, 2015; Barichivich *et al*., 2018). Future analysis would be useful in understanding the response of hydrometeorological parameters to the different ENSO types in the Amazon basin through an intercomparison analysis. Ideally this would incorporate both spatially defined (e.g. East Pacific and central Pacific El Niños) and variable specific indices such as the OLR defined events. Such work has already begun for extreme precipitation events in South America (Tedeschi *et al*., 2016), summer rainfall over Peru (Sulca *et al*., 2018) and recent droughts in the Amazon basin (Jimenez *et al*., 2019).

6.4 | Impact of indices on forecast skill

Understanding how different modes of climate variability affect rainfall and river discharge in the Amazon basin could indicate that a realistic representation of these modes is an important component for a climate model that aims to simulate flooding in the Amazon. Hence, it is important to know how well models can capture particular climate features, in addition to knowing by how much does the inclusion of capturing climate features (e.g. phases of MJO) in the initial conditions of forecasts improve performance. Previous research at the European Centre for Medium-Range Weather Forecasts (ECMWF) has focused on how the incorporation of observations during active phases of the Madden–Julian Oscillation (MJO) in the initial conditions of forecasts influences the ability to predict meteorological variables in the Northern Hemisphere (Vitart and Molteni, 2016). A similar analysis would be useful for the Amazon to explore whether or not hydrological forecasts of river flow have increased skill during particular phases of the ENSO, the tropical Atlantic or the MJO. If model performance were found to increase for particular climate conditions, humanitarian managers using information from climate models could have more confidence in the forecasts when using such information for decision-making. Moreover, knowing how different models capture large-scale climate features and if, or not, they increase forecast performance can provide a useful input when trying to eliminate unrealistic models and focus on more realistic models for certain variables.

6.5 | Calculating flood probabilities

The ultimate question, particular with regards to decision-making, would be how much higher are the chances of flooding if a climate mode is in a particular phase. For example, by how much does the likelihood of flooding increase in the Amazon during the cold phase of

the ENSO? Similar to the global scale analysis performed by Emerton *et al*. (2017) for the ENSO, it would be a worthwhile task to undertake a similar analysis specifically for the Amazon basin and to extend it to include a range of indices such as the TNA, TSA and MJO. Within such a study, it would be worth considering the probabilities of both single and combined phases of different indices (e.g. just La Niña and warm TSA and La Niña combined), in addition to calculating the probabilities for different types of the ENSO events (e.g. east Pacific versus central Pacific). Doing so could provide added predictability over the use of a single index as a predictor (Emerton *et al*., 2019), and would provide a more complete picture of a range of different climate scenarios. Finally, the analysis could be further broken down to consider the probabilities of exceeding a particular percentile or threshold of river flows for different intensities of climate phases (e.g. for weak, medium or strong La Niña events). Again, although complicated by the limited number of events, this analysis could help one to understand some of the uncertainties surrounding the impacts of climate indices. For instance, Nobre *et al*. (2019) provide the example of several countries taking preparedness measures during the strong 2015–2016 El Niño event for expected flooding associated with the elevated probability of flooding during the warm phase of the ENSO. In this instance, Peru (northern regions outside of the Amazon) experienced severe floods, while no flooding occurred in Japan, despite the elevated probability during this particular ENSO phase. Extending the analysis to consider the intensity, spatial complexities and combinations of various climate indices could allow further insights into the uncertainties surrounding the influence of climate phases on the likelihood of floods in certain locations. This work would ideally be supplemented to consider the socioeconomic impacts to different phases of climate (Di Baldassarre *et al*., 2015), as the recording of floods also depends on a region's ability to mitigate, cope and recover.

ACKNOWLEDGEMENTS

This work was supported by the Natural Environment Research Council (NERC) as part of the SCENARIO Doctoral Training Partnership (grant agreement number NE/L002566/1). The first author is grateful for additional travel support and funding provided by the Red Cross Red Crescent Climate Centre. A special thanks to the observational and national services, SO-HYBAM, SENAMHI, ANA, INAMHI and IRD, for providing observed river discharge data and advice throughout the writing of the paper. For access to river flow data please contact the Institute of Research for Development (IRD). The authors declare that they have no conflict of interest.

ORCID

Jamie Towner https://orcid.org/0000-0003-3999-0040

REFERENCES

Aalto, R., Maurice-Bourgoin, L., Dunne, T., Montgomery, D.R., Nittrouer, C.A. and Guyot, J.L. (2003) Episodic sediment accumulation on Amazonian flood plains influenced by El Nino/Southern Oscillation. *Nature*, 425(6957), 493–497. https://doi.org/10.1038/nature02002.

Alfieri, L., Burek, P., Dutra, E., Krzeminski, B., Muraro, D., Thielen, J. and Pappenberger, F. (2013) GloFAS-global ensemble streamflow forecasting and flood early warning. *Hydrology and Earth System Sciences*, 17(3), 1161–1175. https://doi.org/10.5194/hess-17-1161-2013.

Alfieri, L., Bisselink, B., Dottori, F., Naumann, G., de Roo, A., Salamon, P., Wyser, K. and Feyen, L. (2017) Global projections of river flood risk in a warmer world. *Earth's Future*, 5(2), 171–182. https://doi.org/10.1002/2016EF000485.

Alfieri, L., Cohen, S., Galantowicz, J., Schumann, G.J., Trigg, M. A., Zsoter, E., Prudhomme, C., Kruczkiewicz, A., Coughlan de Perez, E., Flamig, Z., Rudari, R., Wu, H., Alder, R.F., Brakenridge, G., Kettner, A., Weerts, A., Matgen, P., Islam, S.A.K.M. and Salamon, P. (2018) A global network for operational flood risk reduction. *Environmental Science & Policy*, 84, 149–158. https://doi.org/10.1016/j.envsci.2018.03.014.

Andreoli, R.V., de Souza, R.A.F., Kayano, M.T. and Candido, L.A. (2012) Seasonal anomalous rainfall in the central and eastern Amazon and associated anomalous oceanic and atmospheric patterns. *International Journal of Climatology*, 32(8), 1193–1205. https://doi.org/10.1002/joc.2345.

Aragão, L.E., Anderson, L.O., Fonseca, M.G., Rosan, T.M., Vedovato, L.B., Wagner, F.H., Silva, C.V.J., Silva Junior, C.H.L., Arai, E., Aguiar, A.P., Barlow, J., Berenguer, E., Deeter, M.N., Domingues, L.G., Gloor, M., Malhi, Y., Marengo, J.A., Miller, J. B., Phillips, O.L. and Saatchi, S. (2018) 21st century drought-related fires counteract the decline of Amazon deforestation carbon emissions. *Nature Communications*, 9(1), 1–12. https://doi.org/10.1038/s41467-017-02771-y.

Barichivich, J., Gloor, E., Peylin, P., Brienen, R.J., Schöngart, J., Espinoza, J.C. and Pattnayak, K.C. (2018) Recent intensification of Amazon flooding extremes driven by strengthened Walker circulation. *Science Advances*, 4(9), eaat8785. https://doi.org/10.1126/sciadv.aat8785.

Barnston, A.G., van den Dool, H.M., Zebiak, S.E., Barnett, T.P., Ji, M., Rodenhuis, D.R., Cane, M.A., Leetmaa, A., Graham, N.E., Ropelewski, C.R., Kousky, V.E., O'Lenic, E.A. and Livezey, R.A. (1994) Long-lead seasonal forecasts—where do we stand? *Bulletin of the American Meteorological Society*, 75(11), 2097–2114. https://doi.org/10.1175/1520-0477(1994)075<2097:LLSFDW>2.0.CO;2.

Bazo, J [homepage on the internet]. (2018) Assessing Flood Preparedness in the Peruvian Amazon. [Cited June 12, 2019]. Available at: https://www.climatecentre.org/news/965/assessing-flood-preparedness-in-the-peruvian-amazon-basin. Last accessed June 14, 2018 [Accessed 20th February 2020].

Bjerknes, J. (1969) Atmospheric teleconnections from the Equatorial Pacific. *Monthly Weather Review*, 97(3), 163–172. https://doi.org/10.1175/1520-0493(1969)097<0163:ATFTEP>2.3.CO;2.

Booth, B.B., Dunstone, N.J., Halloran, P.R., Andrews, T. and Bellouin, N. (2012) Aerosols implicated as a prime driver of twentieth-century North Atlantic climate variability. *Nature*, 484(7393), 228–232. https://doi.org/10.1038/nature10946.

Bourrel, L., Phillips, L. and Moreau, S. (2009) The dynamics of floods in the Bolivian Amazon Basin. *Hydrological Processes*, 23 (22), 3161–3167. https://doi.org/10.1002/hyp.7384.

Builes-Jaramillo, A., Marwan, N., Poveda, G. and Kurths, J. (2018) Nonlinear interactions between the Amazon River basin and the tropical North Atlantic at interannual timescales. *Climate Dynamics*, 50(7–8), 2951–2969. https://doi.org/10.1007/s00382-017-3785-8.

Bunge, L. and Clarke, A.J. (2009) A verified estimation of the El Niño index Niño-3.4 since 1877. *Journal of Climate*, 22(14), 3979–3992. https://doi.org/10.1175/2009JCLI2724.1.

Cai, W., Santoso, A., Wang, G., Yeh, S.W., An, S.I., Cobb, K.M., Collins, M., Guilyardi, E., Jin, F.F., Kug, J.-S., Lengaigne, M., McPhaden, M.J., Takahashi, K., Timmermann, A., Vecchi, G., Watanabe, M. and Wu, L. (2015) ENSO and greenhouse warming. *Nature Climate Change*, 5(9), 849–859. https://doi.org/10.1038/nclimate2743.

Cai, W., McPhaden, M.J., Grimm, A.M., Rodrigues, R.R., Taschetto, A.S., Garreaud, R.D., Dewitte, B., Poveda, G., Ham, Y.-G., Santoso, A., Ng, B., Anderson, W., Wang, G., Geng, T., Marengo, J.A., Alves, L.M., Osman, S.L., Wu, L., Karamperidou, C., Takahashi, K. and Vera, C. (2020) Climate impacts of the El Niño–Southern Oscillation on South America. *Nature Reviews Earth & Environment*, 1(4), 215–231. https://doi.org/10.1038/s43017-020-0040-3.

Callède, J., Guyot, J.L., Ronchail, J., L'Hôte, Y., Niel, H. and de Oliveira, E. (2004) Evolution du débit de l'Amazone à Óbidos de 1903 à 1999/Evolution of the River Amazon's discharge at Óbidos from 1903 to 1999. *Hydrological Sciences Journal*, 49(1), 85–97. https://doi.org/10.1623/hysj.49.1.85.53992.

Callède, J., Cochonneau, G., Alves, F.V., Guyot, J.-L., Guimarães, V.S. and De Oliveira, E. (2010) Les apports en eau de l'Amazone à l'Océan Atlantique. *Revue des sciences de l'eau/Journal of Water Science*, 23(3), 247–273. https://doi.org/10.7202/044688ar.

Carvalho, L.M., Jones, C. and Liebmann, B. (2004) The South Atlantic convergence zone: intensity, form, persistence, and relationships with intraseasonal to interannual activity and extreme rainfall. *Journal of Climate*, 17(1), 88–108. https://doi.org/10.1175/1520-0442(2004)017<0088:TSACZI>2.0.CO;2.

CEPAL. (2008) *Evaluacion del Impacto Acumulado y Adicional Ocacionado por la Niña 2008 en Bolivia, Ministerio de Planificación del Desarrollo (MPD) de Bolivia*. La Paz-Bolivia: Secretaría Ejecutiva de la Comisión Económica para América Latina y el Caribe (CEPAL).

Chikamoto, Y., Timmermann, A., Luo, J.J., Mochizuki, T., Kimoto, M., Watanabe, M., Ishii, M., Xie, S.P. and Jin, F.F. (2015) Skilful multi-year predictions of tropical trans-basin climate variability. *Nature Communications*, 6, 6869. https://doi.org/10.1038/ncomms7869.

Chiodi, A.M. and Harrison, D.E. (2013) El Niño impacts on seasonal US atmospheric circulation, temperature, and precipitation anomalies: the OLR-event perspective. *Journal of Climate*, 26(3), 822–837. https://doi.org/10.1175/JCLI-D-12-00097.1.

Chiodi, A.M. and Harrison, D.E. (2015) Global seasonal precipitation anomalies robustly associated with El Niño and La Niña events—an OLR perspective. *Journal of Climate*, 28(15), 6133–6159. https://doi.org/10.1175/JCLI-D-14-00387.1.

Cloke, H.L. and Pappenberger, F. (2009) Ensemble flood forecasting: a review. *Journal of Hydrology*, 375(3), 613–626. https://doi.org/10.1016/j.jhydrol.2009.06.005.

Cools, J., Innocenti, D. and O'Brien, S. (2016) Lessons from flood early warning systems. *Environmental Science & Policy*, 58, 117–122. https://doi.org/10.1016/j.envsci.2016.01.006.

Coughlan de Perez, E., van den Hurk, B.J.J.M., Van Aalst, M.K., Jongman, B., Klose, T. and Suarez, P. (2015) Forecast-based financing: an approach for catalyzing humanitarian action based on extreme weather and climate forecasts. *Natural Hazards and Earth System Sciences*, 15(4), 895–904. https://doi.org/10.5194/nhess-15-895-2015.

Coumou, D. and Rahmstorf, S. (2012) A decade of weather extremes. *Nature Climate Change*, 2(7), 491–496. https://doi.org/10.1038/NCLIMATE1452.

Cox, P.M., Harris, P.P., Huntingford, C., Betts, R.A., Collins, M., Jones, C.D., Jupp, T.E., Marengo, J.A. and Nobre, C.A. (2008) Increasing risk of Amazonian drought due to decreasing aerosol pollution. *Nature*, 453(7192), 212–215. https://doi.org/10.1038/nature06960.

Dartmouth Flood Observatory [homepage on the internet]. (2018) Global Active Archive of Large Flood Events. [Cited 2017 June 14]. Available at: http://www.dartmouovth.edu/~floods/Archives/index.html. [Accessed 14th June 2018].

Davidson, E.A., de Araújo, A.C., Artaxo, P., Balch, J.K., Brown, I.F., Bustamante, M.M.C., Coe, M.T., DeFries, R.S., Keller, M., Longo, M., Munger, J.W., Schroeder, W., Soares-Filho, B.S., Carlos, M. and Wofsy, S.C. (2012) The Amazon basin in transition. *Nature*, 481(7381), 321–328. https://doi.org/10.1038/nature10717.

De Linage, C., Famiglietti, J.S. and Randerson, J.T. (2014) Statistical prediction of terrestrial water storage changes in the Amazon Basin using tropical Pacific and North Atlantic Sea surface temperature anomalies. *Hydrology and Earth System Sciences*, 18(6), 2089–2102. https://doi.org/10.5194/hess-18-2089-2014.

De Souza, E.B. and Ambrizzi, T. (2006) Modulation of the intraseasonal rainfall over tropical Brazil by the Madden–Julian oscillation. *International Journal of Climatology: A Journal of the Royal Meteorological Society*, 26(13), 1759–1776 10.1002/joc.1331.

Deser, C., Alexander, M.A., Xie, S.P. and Phillips, A.S. (2010) Sea surface temperature variability: patterns and mechanisms. *Annual review of marine science*, 2, 115–143. https://doi.org/10.1146/annurev-marine-120408-151453.

Dettinger, M.D. and Diaz, H.F. (2000) Global characteristics of stream flow seasonality and variability. *Journal of Hydrometeorology*, 1(4), 289–310. https://doi.org/10.1175/1525-7541(2000)001<0289:GCOSFS>2.0.CO;2.

Di Baldassarre, G., Viglione, A., Carr, G., Kuil, L., Yan, K., Brandimarte, L. and Blöschl, G. (2015) Debates—perspectives on socio-hydrology: capturing feedbacks between physical and social processes. *Water Resources Research*, 51(6), 4770–4781. https://doi.org/10.1002/2014WR016416.

ECMWF [homepage on the internet]. (2020) ERA-5 Land [cited 2020 March 02]. Available at: https://www.ecmwf.int/en/era5-land [Accessed 2nd March 2020].

Emerton, R.E., Stephens, E.M., Pappenberger, F., Pagano, T.C., Weerts, A.H., Wood, A.W., Salamon, P., Brown, J.D., Hjerdt, N., Donnelly, C., Baugh, C.A. and Cloke, H.L. (2016) Continental and global scale flood forecasting systems. *Wiley Interdisciplinary Reviews: Water*, 3(3), 391–418. https://doi.org/10.1002/wat2.1137.

Emerton, R.E., Cloke, H.L., Stephens, E.M., Zsoter, E., Woolnough, S.J. and Pappenberger, F. (2017) Complex picture for likelihood of ENSO-driven flood hazard. *Nature Communications*, 8, 14796. https://doi.org/10.1038/ncomms14796.

Emerton, R.E., Stephens, E.M. and Cloke, H.L. (2019) What is the most useful approach for forecasting hydrological extremes during El Niño? *Environmental Research Communications*, 1(3), 031002. https://doi.org/10.1088/2515-7620/ab114e.

Enfield, D.B. (1996) Relationships of inter-American rainfall to tropical Atlantic and Pacific SST variability. *Geophysical Research Letters*, 23(23), 3305–3308. https://doi.org/10.1029/96GL03231.

Enfield, D.B. and Mayer, D.A. (1997) Tropical Atlantic Sea surface temperature variability and its relation to El Niño-southern oscillation. *Journal of Geophysical Research: Oceans*, 102(C1), 929–945. https://doi.org/10.1029/96JC03296.

Enfield, D.B., Mestas-Nuñez, A.M., Mayer, D.A. and Cid-Serrano, L. (1999) How ubiquitous is the dipole relationship in tropical Atlantic Sea surface temperatures? *Journal of Geophysical Research: Oceans*, 104(C4), 7841–7848. https://doi.org/10.1029/1998JC900109.

Enfield, D.B., Mestas-Nuñez, A.M. and Trimble, P.J. (2001) The Atlantic multidecadal oscillation and its relation to rainfall and river flows in the continental US. *Geophysical Research Letters*, 28(10), 2077–2080. https://doi.org/10.1029/2000GL012745.

Espinoza, J.C.E., Guyot, J.L., Ronchail, J., Cochonneau, G., Filizola, N., Fraizy, P., Labat, D., Oliveira, E.D., Ordoñez, J.J. and Vauchel, P. (2009a) Contrasting regional discharge evolutions in the Amazon basin (1974–2004). *Journal of Hydrology*, 375(3–4), 297–311. https://doi.org/10.1016/j.jhydrol.2009.03.004.

Espinoza, J.C.E., Ronchail, J., Guyot, J.L., Cochonneau, G., Naziano, F., Lavado, W., Oliveira, D.E., Pombosa, R. and Vauchel, P. (2009b) Spatio-temporal rainfall variability in the Amazon basin countries (Brazil, Peru, Bolivia, Colombia, and Ecuador). *International Journal of Climatology*, 29(11), 1574–1594. https://doi.org/10.1002/joc.1791.

Espinoza, J.C.E., Ronchail, J., Guyot, J.L., Junquas, C., Drapeau, G., Martinez, J.M., Santini, W., Vauchel, P., Lavado, W., Ordoñez, J. and Espinoza, R. (2012) From drought to flooding: understanding the abrupt 2010–11 hydrological annual cycle in the Amazonas River and tributaries. *Environmental Research Letters*, 7(2), 024008. https://doi.org/10.1088/1748-9326/7/2/024008.

Espinoza, J.C.E., Ronchail, J., Frappart, F., Lavado, W., Santini, W. and Guyot, J.L. (2013) The major floods in the Amazonas River and tributaries (Western Amazon basin) during the 1970–2012 period: a focus on the 2012 flood. *Journal of Hydrometeorology*, 14(3), 1000–1008. https://doi.org/10.1175/JHM-D-12-0100.1.

Espinoza, J.C.E., Marengo, J.A., Ronchail, J., Carpio, J.M., Flores, L.N. and Guyot, J.L. (2014) The extreme 2014 flood in South-Western Amazon basin: the role of tropical–subtropical South Atlantic SST gradient. *Environmental Research Letters*, 9(12), 124007. https://doi.org/10.1088/1748-9326/9/12/124007.

Espinoza, J.C., Segura, H., Ronchail, J., Drapeau, G. and Gutierrez-Cori, O. (2016) Evolution of wet-day and dry-day frequency in the western Amazon basin: relationship with atmospheric circulation and impacts on vegetation. *Water Resources Research*, 52(11), 8546–8560. https://doi.org/10.1002/2016WR019305.

Espinoza, J.C., Ronchail, J., Marengo, J.A. and Segura, H. (2019) Contrasting north–south changes in Amazon wet-day and dry-day frequency and related atmospheric features (1981–2017). *Climate Dynamics*, 52(9–10), 5413–5430. https://doi.org/10.1007/s00382-018-4462-2.

Figueroa, S.N. and Nobre, C.A. (1990) Precipitation distribution over central and western tropical South America. *Climanalise*, 5(6), 36–45.

Filizola, N., Latrubesse, E.M., Fraizy, P., Souza, R., Guimarães, V. and Guyot, J.L. (2014) Was the 2009 flood the most hazardous or the largest ever recorded in the Amazon? *Geomorphology*, 215, 99–105. https://doi.org/10.1016/j.geomorph.2013.05.028.

Foley, J.A., Botta, A., Coe, M.T. and Costa, M.H. (2002) El Niño–southern oscillation and the climate, ecosystems and rivers of Amazonia. *Global Biogeochemical Cycles*, 16(4), 79-1–79-20. https://doi.org/10.1029/2002GB001872.

Forecast-based-financing.org [homepage on the internet]. (2019) Forecast based Financing. [Cited 2020 February 18]. Available at: https://www.forecast-based-financing.org/wp-content/uploads/2019/01/Brochure-Tecnico-Iquitos-english.pdf. [Accessed 20th February 2020].

Frauen, C., Dommenget, D., Tyrrell, N., Rezny, M. and Wales, S. (2014) Analysis of the nonlinearity of El Niño–southern oscillation teleconnections. *Journal of Climate*, 27(16), 6225–6244. https://doi.org/10.1175/JCLI-D-13-00757.1.

Fu, R., Zhu, B. and Dickinson, R.E. (1999) How do atmosphere and land surface influence seasonal changes of convection in the tropical Amazon? *Journal of Climate*, 12(5), 1306–1321. https://doi.org/10.1175/1520-0442(1999)012<1306:HDAALS>2.0.CO;2.

García-García, D. and Ummenhofer, C.C. (2015) Multidecadal variability of the continental precipitation annual amplitude driven by AMO and ENSO. *Geophysical Research Letters*, 42(2), 526–535. https://doi.org/10.1002/2014GL062451.

García-Serrano, J., Cassou, C., Douville, H., Giannini, A. and Doblas-Reyes, F.J. (2017) Revisiting the ENSO teleconnection to the tropical North Atlantic. *Journal of Climate*, 30(17), 6945–6957. https://doi.org/10.1175/JCLI-D-16-0641.1.

Gautier, E., Brunstein, D., Vauchel, P., Roulet, M., Fuertes, O., Guyot, J.L., Darrozzes, J. and Bourrel, L. (2006) Temporal relations between meander deformation, water discharge and sediment fluxes in the floodplain of the Rio Beni (Bolivian Amazonia). *Earth Surface Processes and Landforms*, 32(2), 230–248. https://doi.org/10.1002/esp.1394.

Geng, T., Yang, Y. and Wu, L. (2019) On the mechanisms of Pacific decadal oscillation modulation in a warming climate. *Journal of Climate*, 32, 1443–1459. https://doi.org/10.1175/JCLI-D-18-0337.1.

Gloor, M.R.J.W., Brienen, R.J., Galbraith, D., Feldpausch, T.R., Schöngart, J., Guyot, J.L., Espinoza, J.C., Llyod, J. and Phillips, O.L. (2013) Intensification of the Amazon hydrological cycle over the last two decades. *Geophysical Research Letters*, 40(9), 1729–1733. https://doi.org/10.1002/grl.50377.

Grimm, A.M. and Tedeschi, R.G. (2009) ENSO and extreme rainfall events in South America. *Journal of Climate*, 22(7), 1589–1609. https://doi.org/10.1175/2008JCLI2429.1.

Ham, Y.G., Kug, J.S., Park, J.Y. and Jin, F.F. (2013) Sea surface temperature in the north tropical Atlantic as a trigger for El Niño/southern oscillation events. *Nature Geoscience*, 6(2), 112–116. https://doi.org/10.1038/ngeo1686.

Hill, K.J., Taschetto, A.S. and England, M.H. (2009) South American rainfall impacts associated with inter-El Niño variations. *Geophysical Research Letters*, 36(19), L19702. https://doi.org/10.1029/2009GL040164.

Hill, K.J., Taschetto, A.S. and England, M.H. (2011) Sensitivity of South American summer rainfall to tropical Pacific Ocean SST anomalies. *Geophysical Research Letters*, 38(1). https://doi.org/10.1029/2010GL045571.

Hirabayashi, Y., Mahendran, R., Koirala, S., Konoshima, L., Yamazaki, D., Watanabe, S., Kim, H. and Kanae, S. (2013) Global flood risk under climate change. *Nature Climate Change*, 3(9), 816–821. https://doi.org/10.1038/nclimate1911.

IFRC [homepage on the internet]. (2012) DREF operation update Peru: Floods. [Cited 2017 June 08]. Available at: https://reliefweb.int/sites/reliefweb.int/files/resources/MDRPE005du1.pdf [Accessed 08th June 2017].

Jimenez, J.C., Marengo, J.A., Alves, L.M., Sulca, J.C., Takahashi, K., Ferrett, S. and Collins, M. (2019) The role of ENSO flavours and TNA on recent droughts over Amazon forests and the Northeast Brazil region. *International Journal of Climatology*, 1–20. https://doi.org/10.1002/joc.6453.

Jones, C. and Carvalho, L.M. (2018) The influence of the Atlantic multidecadal oscillation on the eastern Andes low-level jet and precipitation in South America. *npj Climate and Atmospheric Science*, 1(1), 40. https://doi.org/10.1038/s41612-018-0050-8.

Jones, C., Waliser, D.E., Lau, K.M. and Stern, W. (2004) Global occurrences of extreme precipitation and the Madden–Julian oscillation: observations and predictability. *Journal of Climate*, 17(23), 4575–4589. https://doi.org/10.1175/3238.1.

Kayano, M.T. and Andreoli, R.V. (2007) Relations of south American summer rainfall interannual variations with the Pacific decadal oscillation. *International Journal of Climatology*, 27(4), 531–540. https://doi.org/10.1002/joc.1417.

Kayano, M.T. and Capistrano, V.B. (2013) How the Atlantic multidecadal oscillation (AMO) modifies the ENSO influence on the South American rainfall. *International Journal of Climatology*, 34(1), 162–178. https://doi.org/10.1002/joc.3674.

Kayano, M.T., Andreoli, R.V. and Souza, R.A.F.D. (2019) El Niño–southern oscillation related teleconnections over South America under distinct Atlantic multidecadal oscillation and Pacific Interdecadal oscillation backgrounds: La Niña. *International Journal of Climatology*, 39(3), 1359–1372. https://doi.org/10.1002/joc.5886.

Kerr, R.A. (2000) A North Atlantic climate pacemaker for the centuries. *Science*, 288(5473), 1984–1985. https://doi.org/10.1126/science.288.5473.1984.

Kobayashi, S., Ota, Y., Harada, Y., Ebita, A., Moriya, M., Onoda, H., Onogi, K., Kamahori, H., Kobayashi, C., Endo, H., Miyaoka, K. and Takahashi, K. (2015) The JRA-55 reanalysis: general specifications and basic characteristics. *Journal of the Meteorological Society of Japan. Ser. II*, 93(1), 5–48. https://doi.org/10.2151/jmsj.2015-001.

Lagos, P., Silva, Y., Nickl, E. and Mosquera, K. (2008) El Niño? Related precipitation variability in Perú. *Advances in Geosciences*, 14, 231–237. https://doi.org/10.5194/adgeo-14-231-2008.

Langerwisch, F., Rost, S., Gerten, D., Poulter, B., Rammig, A. and Cramer, W. (2013) Potential effects of climate change on inundation patterns in the Amazon Basin. *Hydrology and Earth System Sciences*, 17(6), 2247–2262. https://doi.org/10.5194/hess-17-2247-2013.

Langill, J.C. and Abizaid, C. (2019) What is a bad flood? Local perspectives of extreme floods in the Peruvian Amazon. *Ambio*, 49, 1–14. https://doi.org/10.1007/s13280-019-01278-8.

Laraque, A., Ronchail, J., Cochonneau, G., Pombosa, R. and Guyot, J.L. (2007) Heterogeneous distribution of rainfall and discharge regimes in the Ecuadorian Amazon basin. *Journal of Hydrometeorology*, 8(6), 1364–1381. https://doi.org/10.1175/2007JHM784.1.

Laraque, A., Bernal, C., Bourrel, L., Darrozes, J., Christophoul, F., Armijos, E., Fraizy, P., Pombosa, R. and Guyot, J.L. (2009) Sediment budget of the Napo river, Amazon basin, Ecuador and Peru. *Hydrological Processes: An International Journal*, 23(25), 3509–3524. https://doi.org/10.1002/hyp.7463.

Lavado, W.S., Ronchail, J., Labat, D., Espinoza, J.C. and Guyot, J.L. (2012) Basin-scale analysis of rainfall and runoff in Peru (1969–2004): Pacific, Titicaca and Amazonas drainages. *Hydrological Sciences Journal*, 57(4), 625–642. https://doi.org/10.1080/02626667.2012.672985.

Lavado, W.S., Labat, D., Ronchail, J., Espinoza, J.C. and Guyot, J.L. (2013) Trends in rainfall and temperature in the Peruvian Amazon–Andes basin over the last 40 years (1965–2007). *Hydrological Processes*, 27(20), 2944–2957. https://doi.org/10.1002/hyp.9418.

Le Cointe, P. (1935) Les crues annuelles de l'Amazone et les récentes modifications de leur régime. *Annales de Géogr.*, 44, 614–619.

Lee, D., Ward, P. and Block, P. (2018) Attribution of large-scale climate patterns to seasonal peak-flow and prospects for prediction globally. *Water Resources Research*, 54(2), 916–938. https://doi.org/10.1002/2017WR021205.

Liebmann, B. and Marengo, J. (2001) Interannual variability of the rainy season and rainfall in the Brazilian Amazon Basin. *Journal of Climate*, 14(22), 4308–4318. https://doi.org/10.1175/1520-0442(2001)014<4308:IVOTRS>2.0.CO;2.

Liebmann, B., Kiladis, G.N., Vera, C.S., Saulo, A.C. and Carvalho, L.M. (2004) Subseasonal variations of rainfall in South America in the vicinity of the low-level jet east of the Andes and comparison to those in the South Atlantic convergence zone. *Journal of Climate*, 17(19), 3829–3842. https://doi.org/10.1175/1520-0442(2004)017<3829:SVORIS>2.0.CO;2.

Lopez, M.G., Di Baldassarre, G. and Seibert, J. (2017) Impact of social preparedness on flood early warning systems. *Water Resources Research*, 53(1), 522–534. https://doi.org/10.1002/2016WR019387.

Madden, R.A. and Julian, P.R. (1971) Detection of a 40–50 day oscillation in the zonal wind in the tropical Pacific. *Journal of the Atmospheric Sciences*, 28(5), 702–708. https://doi.org/10.1175/1520-0469(1971)028<0702:DOADOI>2.0.CO;2.

Madden, R.A. and Julian, P.R. (1972) Description of global-scale circulation cells in the tropics with a 40–50 day period. *Journal of the Atmospheric Sciences*, 29(6), 1109–1123. https://doi.org/10.1175/1520-0469(1972)029<1109:DOGSCC>2.0.CO;2.

Madden, R.A. and Julian, P.R. (1994) Observations of the 40–50-day tropical oscillation—a review. *Monthly Weather Review*, 122(5), 814–837. https://doi.org/10.1175/1520-0493(1994)122<0814:OOTDTO>2.0.CO;2.

Makarieva, A.M. and Gorshkov, V.G. (2007) Biotic pump of atmospheric moisture as driver of the hydrological cycle on land. *Hydrology and Earth System Sciences*, 11, 1013–1033. https://doi.org/10.5194/hess-11-1013-2007.

Mantua, N.J. and Hare, S.R. (2002) The Pacific decadal oscillation. *Journal of Oceanography*, 58(1), 35–44. https://doi.org/10.1023/A:1015820616384.

Mantua, N.J., Hare, S.R., Zhang, Y., Wallace, J.M. and Francis, R.C. (1997) A Pacific interdecadal climate oscillation with impacts on salmon production. *Bulletin of the American Meteorological Society*, 78(6), 1069–1080. https://doi.org/10.1175/1520-0477(1997)078<1069:APICOW>2.0.CO;2.

Marengo, J.A. (1992) Interannual variability of surface climate in the Amazon basin. *International Journal of Climatology*, 12(8), 853–863. https://doi.org/10.1002/joc.3370120808.

Marengo, J.A. and Espinoza, J.C. (2016) Extreme seasonal droughts and floods in Amazonia: causes, trends and impacts. *International Journal of Climatology*, 36(3), 1033–1050. https://doi.org/10.1002/joc.4420.

Marengo, J.A. and Nobre, C.A. (2001) General characteristics and variability of climate in the Amazon Basin and its links to the global climate system. In: McClain, M.E., Victoria, R.L. and Richey, J.E. (Eds.) *The Biogeochemistry of the Amazon Basin*. Oxford: Oxford Univ. Press.

Marengo, J.A., Druyan, L.M. and Hastenrath, S. (1993) Observational and modelling studies of Amazonia interannual climate variability. *Climatic Change*, 23(3), 267–286. https://doi.org/10.1007/BF01091619.

Marengo, J.A., Tomasella, J. and Uvo, C.R. (1998) Trends in streamflow and rainfall in tropical South America: Amazonia, eastern Brazil, and northwestern Peru. *Journal of Geophysical Research: Atmospheres*, 103(D2), 1775–1783. https://doi.org/10.1029/97JD02551.

Marengo, J.A., Liebmann, B., Kousky, V.E., Filizola, N.P. and Wainer, I.C. (2001) Onset and end of the rainy season in the Brazilian Amazon Basin. *Journal of Climate*, 14(5), 833–852. https://doi.org/10.1175/1520-0442(2001)014<0833:OAEOTR>2.0.CO;2.

Marengo, J.A., Nobre, C.A., Tomasella, J., Cardoso, M.F. and Oyama, M.D. (2008) Hydro-climatic and ecological behaviour of the drought of Amazonia in 2005. *Philosophical Transactions of the Royal Society B: Biological Sciences*, 363(1498), 1773–1778. https://doi.org/10.1098/rstb.2007.0015.

Marengo, J.A., Tomasella, J., Alves, L.M., Soares, W.R. and Rodriguez, D.A. (2011) The drought of 2010 in the context of historical droughts in the Amazon region. *Geophysical Research Letters*, 38(12), 1–5. https://doi.org/10.1029/2011GL047436.

Marengo, J.A., Tomasella, J., Soares, W.R., Alves, L.M. and Nobre, C.A. (2012) Extreme climatic events in the Amazon basin. *Theoretical and Applied Climatology*, 107(1–2), 73–85. https://doi.org/10.1007/s00704-011-0465-1.

Marengo, J.A., Alves, L.M., Soares, W.R., Rodriguez, D.A., Camargo, H., Riveros, M.P. and Pabló, A.D. (2013a) Two contrasting severe seasonal extremes in tropical South America in 2012: flood in Amazonia and drought in Northeast Brazil. *Journal of Climate*, 26(22), 9137–9154. https://doi.org/10.1175/JCLI-D-12-00642.1.

Marengo, J.A., Borma, L.S., Rodríguez, D.A., Pinho, P., Soares, W.R. and Alves, L.M. (2013b) Recent extremes of drought and flooding in Amazonia: vulnerabilities and human adaptation. *American Journal of Climate Change*, 2(02), 87–96. https://doi.org/10.4236/ajcc.2013.22009.

Marengo, J.A., Williams, E.R., Alves, L.M., Soares, W.R. and Rodriguez, D.A. (2016) Extreme seasonal climate variations in the Amazon basin: droughts and floods. In: *Interactions between Biosphere, Atmosphere and Human Land Use in the Amazon Basin*, Vol. 36. Berlin, Heidelberg: Springer, pp. 55–76. https://doi.org/10.1002/joc.4420.

Marengo, J.A., Souza, C.M., Jr., Thonicke, K., Burton, C., Halladay, K., Betts, R., Alves, L.M. and Soares, W.R. (2018) Changes in climate and land use over the amazon region: current and future variability and trends. *Frontiers in Earth Science*, 6(228). https://doi.org/10.3389/feart.2018.00228.

Martín-Rey, M., Polo, I., Rodríguez-Fonseca, B., Losada, T. and Lazar, A. (2018) Is there evidence of changes in tropical Atlantic variability modes under AMO phases in the observational record? *Journal of Climate*, 31(2), 515–536. https://doi.org/10.1175/JCLI-D-16-0459.1.

Matthews, A.J., Hoskins, B.J. and Masutani, M. (2004) The global response to tropical heating in the Madden–Julian oscillation during the northern winter. *Quarterly Journal of the Royal Meteorological Society*, 130(601), 1991–2011. https://doi.org/10.1256/qj.02.123.

McGregor, S., Timmermann, A., Stuecker, M.F., England, M.H., Merrifield, M., Jin, F.F. and Chikamoto, Y. (2014) Recent Walker circulation strengthening and Pacific cooling amplified by Atlantic warming. *Nature Climate Change*, 4(10), 888–892. https://doi.org/10.1038/nclimate2330.

Meade, R.H., Rayol, J.M., Da Conceicão, S.C. and Natividade, J.R. (1991) Backwater effects in the Amazon River basin of Brazil. *Environmental Geology and Water Sciences*, 18(2), 105–114. https://doi.org/10.1007/BF01704664.

Molinier M, Guyot JL, Oliveira E, Guimaraes V. (1996) Les régimes ´ hydrologiques de l'Amazone et de ses affluents. L'hydrologie Tropicale: G´eoscience et outil pour le D´eveloppement 238: 209–222, Paris, Mai 1995. IAHS Publ.

Montini, T.L., Jones, C. and Carvalho, L.M. (2019) The south American low-level jet: A new climatology, variability, and changes. *Journal of Geophysical Research: Atmospheres*, 124, 1200–1218. https://doi.org/10.1029/2018JD029634.

Moura, A.D. and Shukla, J. (1981) On the dynamics of droughts in Northeast Brazil: observations, theory and numerical experiments with a general circulation model. *Journal of the Atmospheric Sciences*, 38(12), 2653–2675. https://doi.org/10.1175/1520-0469(1981)038<2653:OTDODI>2.0.CO;2.

Newman, M., Alexander, M.A., Ault, T.R., Cobb, K.M., Deser, C., Di Lorenzo, E., Mantua, N.J., Miller, A.J., Minobe, S., Nakamura, H., Schneider, N., Vimont, D.J., Phillips, J.S., Scott, J.D. and Smith, C.A. (2016) The Pacific decadal oscillation, revisited. *Journal of Climate*, 29(12), 4399–4442. https://doi.org/10.1175/JCLI-D-15-0508.1.

Nobre, P. and Shukla, J. (1996) Variations of sea surface temperature, wind stress, and rainfall over the tropical Atlantic and South America. *Journal of Climate*, 9(10), 2464–2479. https://doi.org/10.1175/1520-0442(1996)009<2464:VOSSTW>2.0.CO;2.

Nobre, C.A., Sampaio, G., Borma, L.S., Castilla-Rubio, J.C., Silva, J. S. and Cardoso, M. (2016) Land-use and climate change risks in the Amazon and the need of a novel sustainable development paradigm. *Proceedings of the National Academy of Sciences*, 113 (39), 10759–10768. https://doi.org/10.1073/pnas.1605516113.

Nobre, G.G., Jongman, B., Aerts, J.C.J.H. and Ward, P.J. (2017) The role of climate variability in extreme floods in Europe. *Environmental Research Letters*, 12(8), 084012. https://doi.org/10.1088/1748-9326/aa7c22.

Nobre, G.G., Muis, S., Veldkamp, T.I. and Ward, P.J. (2019) Achieving the reduction of disaster risk by better predicting impacts of El Niño and La Niña. *Progress in Disaster Science*, 2, 100022. https://doi.org/10.1016/j.pdisas.2019.100022.

O'Connor, J. E., & Costa, J. E. (2004) The world's largest floods, past and present—their causes and magnitude, U.S. Geological Survey Circular 1254.

O'Reilly, C.H., Huber, M., Woollings, T. and Zanna, L. (2016) The signature of low-frequency oceanic forcing in the Atlantic multidecadal oscillation. *Geophysical Research Letters*, 43(6), 2810–2818. https://doi.org/10.1002/2016GL067925.

Ovando, A., Tomasella, J., Rodriguez, D.A., Martinez, J.M., Siqueira-Junior, J.L., Pinto, G.L.N., Passy, P., Vauchel, P., Noriega, L. and von Randow, C. (2016) Extreme flood events in the Bolivian Amazon wetlands. *Journal of Hydrology: Regional Studies*, 5, 293–308. https://doi.org/10.1016/j.ejrh.2015.11.004.

Paccini, L., Espinoza, J.C., Ronchail, J. and Segura, H. (2018) Intra-seasonal rainfall variability in the Amazon basin related to large-scale circulation patterns: a focus on western Amazon–Andes transition region. *International Journal of Climatology*, 38(5), 2386–2399. https://doi.org/10.1002/joc.5341.

Paiva, R.C.D., Collischonn, W., Bonnet, M.P. and De Gonçalves, L. G.G. (2012) On the sources of hydrological prediction uncertainty in the Amazon. *Hydrology and Earth System Sciences*, 16 (9), 3127–3137. https://doi.org/10.5194/hess-16-3127-2012.

Palmer, T.N. (1993) Extended-range atmospheric prediction and the Lorenz model. *Bulletin of the American Meteorological Society*, 74(1), 49–65. https://doi.org/10.1175/1520-0477(1993)074<0049:ERAPAT>2.0.CO;2.

Palmer, T.N. (1996) Predictability of the atmosphere and oceans: from days to decades. In: *Decadal climate variability*. Berlin, Heidelberg: Springer, pp. 83–155.

Panisset, J.S., Libonati, R., Gouveia, C.M.P., Machado-Silva, F., França, D.A., França, J.R.A. and Peres, L.F. (2018) Contrasting patterns of the extreme drought episodes of 2005, 2010 and 2015 in the Amazon Basin. *International Journal of Climatology*, 38(2), 1096–1104. https://doi.org/10.1002/joc.5224.

Pohl, B. and Matthews, A.J. (2007) Observed changes in the lifetime and amplitude of the Madden–Julian oscillation associated with interannual ENSO sea surface temperature anomalies. *Journal of Climate*, 20(11), 2659–2674. https://doi.org/10.1175/JCLI4230.1.

Poveda G., & Mesa OJ. (1993) Metodologias de prediccion de la hidrologia colombiana considerando el evento de El Nino Oscilaciton del Sur (ENOS), Atmosfera. Sociedad Colombiana de Meteorolog´ıa, 17.

Poveda, G., Alvarez, D.M. and Rueda, O.A. (2011) Hydro-climatic variability over the Andes of Colombia associated with ENSO: a review of climatic processes and their impact on one of the Earth's most important biodiversity hotspots. *Climate Dynamics*, 36(11–12), 2233–2249. https://doi.org/10.1007/s00382-010-0931-y.

Richey, J.E., Nobre, C. and Deser, C. (1989) Amazon River discharge and climate variability: 1903 to 1985. *Science*, 246(4926), 101–103. https://doi.org/10.1126/science.246.4926.101.

Robock, A. (2000) Volcanic eruptions and climate. *Reviews of Geophysics*, 38(2), 191–219. https://doi.org/10.1029/1998RG000054.

Rodier, J.A. and Roche, M. (1984) World catalogue of maximum observed floods. *IAHS Publication*, 143.

Rodrigues, R.R. and McPhaden, M.J. (2014) Why did the 2011–2012 La Niña cause a severe drought in the Brazilian northeast? *Geophysical Research Letters*, 41(3), 1012–1018. https://doi.org/10.1002/2013GL058703.

Ronchail, J. and Gallaire, R. (2006) ENSO and rainfall along the Zongo valley (Bolivia) from the Altiplano to the Amazon basin. *International Journal of Climatology*, 26(9), 1223–1236. https://doi.org/10.1002/joc.1296.

Ronchail, J., Cochonneau, G., Molinier, M., Guyot, J.L., De Miranda Chaves, A.G., Guimarães, V. and De Oliveira, E. (2002) Interannual rainfall variability in the Amazon basin and sea-surface temperatures in the Equatorial Pacific and the tropical Atlantic Oceans. *International Journal of Climatology*, 22 (13), 1663–1686. https://doi.org/10.1002/joc.815.

Ronchail, J., Bourrel, L., Cochonneau, G., Vauchel, P., Phillips, L., Castro, A., Guyot, J.L. and De Oliveira, E. (2005a) Inundations in the Mamore basin (South-Western Amazon—Bolivia) and sea-surface temperature in the Pacific and Atlantic oceans. *Journal of Hydrology*, 302(1–4), 223–238. https://doi.org/10.1016/j.jhydrol.2004.07.005.

Ronchail, J., Labat, D., Callede, J., Cochonneau, G., Guyot, J.L., Filizola, N. and De Oliveira, E. (2005b) Discharge variability within the Amazon basin, regional hydrological impacts of climatic change—hydroclimatic variability. *IAHS Publication*, 296, 21–30.

Ronchail, J., Guyot, J.L., Espinoza, J.C.E., Fraizy, P., Cochonneau, G., De Oliveira, E., Filizola, N. and Ordenez, J.J. (2006) Impact of the Amazon tributaries on major floods at Óbidos. *IAHS Publication*, 308, 220–225.

Rossel, F. (1997) *Influence du Niño sur les régimes pluviométriques de l'equateur*. PhD Thesis, Montpellier University, 289 pp.

Salati, E. and Vose, P.B. (1984) Amazon basin: a system in equilibrium. *Science*, 225(4658), 129–138. https://doi.org/10.1126/science.225.4658.129.

Salati, E., Dall'Olio, A., Matsui, E. and Gat, J.R. (1979) Recycling of water in the Amazon basin: an isotopic study. *Water Resources Research*, 15(5), 1250–1258. https://doi.org/10.1029/WR015i005p01250.

Satyamurty, P., da Costa, C.P.W., Manzi, A.O. and Candido, L.A. (2013) A quick look at the 2012 record flood in the Amazon Basin. *Geophysical Research Letters*, 40(7), 1396–1401. https://doi.org/10.1002/grl.50245.

Schöngart, J. and Junk, W.J. (2007) Forecasting the flood-pulse in Central Amazonia by ENSO-indices. *Journal of Hydrology*, 335 (1–2), 124–132. https://doi.org/10.1016/j.jhydrol.2006.11.005.

Sena, J.A., De Deus, L.A.B., Freitas, M.A.V. and Costa, L. (2012) Extreme events of droughts and floods in Amazonia: 2005 and 2009. *Water Resources Management*, 26(6), 1665–1676. https://doi.org/10.1007/s11269-012-9978-3.

Shimizu, M.H., Ambrizzi, T. and Liebmann, B. (2017) Extreme precipitation events and their relationship with ENSO and MJO

phases over northern South America. *International Journal of Climatology*, 37(6), 2977–2989. https://doi.org/10.1002/joc.4893.

Sigmond, M., Scinocca, J.F., Kharin, V.V. and Shepherd, T.G. (2013) Enhanced seasonal forecast skill following stratospheric sudden warmings. *Nature Geoscience*, 6(2), 98–102. https://doi.org/10.1038/NGEO1698.

Slater, L.J. and Villarini, G. (2017) Evaluating the drivers of seasonal streamflow in the US Midwest. *Water*, 9(9), 695. https://doi.org/10.3390/w9090695.

SO-HYBAM [homepage on the internet]. (2015) Crues 2015 en Amazonie: Les hydrologues du Service d'Observation HYBAM* en état d'alerte. [Cited 2018 July 25]. Available at: https://hybam.obs-mip.fr/note-on-the-flood-of-the-amazon-in-peru-in-2015-2/#more-4690 [Accessed 3rd March 2020].

Sorribas, M.V., Paiva, R.C., Melack, J.M., Bravo, J.M., Jones, C., Carvalho, L., Beighley, E., Forsberg, B. and Costa, M.H. (2016) Projections of climate change effects on discharge and inundation in the Amazon basin. *Climatic Change*, 136(3–4), 555–570. https://doi.org/10.1007/s10584-016-1640-2.

Stephens, E., Day, J.J., Pappenberger, F. and Cloke, H. (2015) Precipitation and floodiness. *Geophysical Research Letters*, 42(23), 10–316. https://doi.org/10.1002/2015GL066779.

Sulca, J., Takahashi, K., Espinoza, J.C., Vuille, M. and Lavado-Casimiro, W. (2018) Impacts of different ENSO flavors and tropical Pacific convection variability (ITCZ, SPCZ) on austral summer rainfall in South America, with a focus on Peru. *International Journal of Climatology*, 38(1), 420–435. https://doi.org/10.1002/joc.5185.

Sutcliffe, J.V. (1987) The use of historical records in flood frequency analysis. *Journal of Hydrology*, 96(1–4), 159–171. https://doi.org/10.1016/0022-1694(87)90150-8.

Tedeschi, R.G., Grimm, A.M. and Cavalcanti, I.F. (2016) Influence of central and east ENSO on precipitation and its extreme events in South America during austral autumn and winter. *International Journal of Climatology*, 36(15), 4797–4814. https://doi.org/10.1002/joc.4670.

Timmermann, A., Okumura, Y., An, S.I., Clement, A., Dong, B., Guilyardi, E., Hu, A., Jungclaus, J.H., Renold, M., Stocker, T.F., Stouffer, R.J., Sutton, R., Xie, S.P. and Yin, J. (2007) The influence of a weakening of the Atlantic meridional overturning circulation on ENSO. *Journal of Climate*, 20(19), 4899–4919. https://doi.org/10.1175/JCLI4283.1.

Tobar, V. and Wyseure, G. (2018) Seasonal rainfall patterns classification, relationship to ENSO and rainfall trends in Ecuador. *International Journal of Climatology*, 38(4), 1808–1819. https://doi.org/10.1002/joc.5297.

Tomasella, J., Borma, L.S., Marengo, J.A., Rodriguez, D.A., Cuartas, L.A., A Nobre, C. and Prado, M.C. (2011) The droughts of 1996–1997 and 2004–2005 in Amazonia: hydrological response in the river main-stem. *Hydrological Processes*, 25(8), 1228–1242. https://doi.org/10.1002/hyp.7889.

Torres, R.R. and Marengo, J.A. (2013) Uncertainty assessments of climate change projections over South America. *Theoretical and Applied Climatology*, 112(1–2), 253–272. https://doi.org/10.1007/s00704-012-0718-7.

Towner, J., Cloke, H.L., Zsoter, E., Flamig, Z., Hoch, J.M., Bazo, J., Coughlan de Perez, E. and Stephens, E.M. (2019) Assessing the performance of global hydrological models for capturing peak river flows in the Amazon basin. *Hydrology and Earth System Sciences*, 23(7), 3057–3080. https://doi.org/10.5194/hess-23-3057-2019.

Trenberth, K.E. (1997) The definition of el nino. *Bulletin of the American Meteorological Society*, 78(12), 2771–2777. https://doi.org/10.1175/1520-0477(1997)078<2771:TDOENO>2.0.CO;2.

Trenberth, K.E. and Stepaniak, D.P. (2001) Indices of el Niño evolution. *Journal of Climate*, 14(8), 1697–1701. https://doi.org/10.1175/1520-0442(2001)014<1697:LIOENO>2.0.CO;2.

Trenberth, K.E., Fasullo, J.T. and Shepherd, T.G. (2015) Attribution of climate extreme events. *Nature Climate Change*, 5(8), 725–730. https://doi.org/10.1038/NCLIMATE2657.

Trigg, M. A. (2010) *Amazon River and floodplain hydrodynamics*. Doctoral thesis, University of Bristol, Bristol.

Trigg, M.A., Wilson, M.D., Bates, P.D., Horritt, M.S., Alsdorf, D.E., Forsberg, B.R. and Vega, M.C. (2009) Amazon flood wave hydraulics. *Journal of Hydrology*, 374(1–2), 92–105. https://doi.org/10.1016/j.jhydrol.2009.06.004.

Utida, G., Cruz, F.W., Etourneau, J., Bouloubassi, I., Schefuß, E., Vuille, M., Novello, V.F., Prado, L.F., Sifeddine, A., Klein, V., Zular, A., Viana, J.C.C. and Turcq, B. (2019) Tropical South Atlantic influence on northeastern Brazil precipitation and ITCZ displacement during the past 2300 years. *Scientific Reports*, 9(1), 1698. https://doi.org/10.1038/s41598-018-38003-6.

Uvo, C.B. and Graham, N.E. (1998) Seasonal runoff forecast for northern South America: A statistical model. *Water Resources Research*, 34(12), 3515–3524. https://doi.org/10.1029/98WR02854.

Uvo, C.B., Tolle, U. and Berndtsson, R. (2000) Forecasting discharge in Amazonia using artificial neural networks. *International Journal of Climatology*, 20(12), 1495–1507. https://doi.org/10.1002/1097-0088(200010)20:12<1495::AID-JOC549>3.0.CO;2-F.

Vauchel, P., Santini, W., Guyot, J.L., Moquet, J.S., Martinez, J.M., Espinoza, J.C., Baby, P., Fuertes, O., Noreiga, L., Puita, O., Sondag, F., Fraizy, P., Armijos, E., Cochonneau, C., Timouk, F., de Oliveira, E., Filizola, N., Molina, J. and Ronchail, J. (2017) A reassessment of the suspended sediment load in the Madeira River basin from the Andes of Peru and Bolivia to the Amazon River in Brazil, based on 10 years of data from the HYBAM monitoring programme. *Journal of Hydrology*, 553, 35–48. https://doi.org/10.1016/j.jhydrol.2017.07.018.

Vitart, F., & Molteni, F. (2016) Simulation of the Madden–Julian oscillation and its impact over Europe in ECMWF's monthly forecasts. *ECMWF Newsletter*, No. 126, ECMWF, Reading, 12–17.

Vuille, M., Bradley, R.S. and Keimig, F. (2000) Climate variability in the Andes of Ecuador and its relation to tropical Pacific and Atlantic sea surface temperature anomalies. *Journal of Climate*, 13(14), 2520–2535. https://doi.org/10.1175/1520-0442(2000)013<2520:CVITAO>2.0.CO;2.

Wang, S., Huang, J., He, Y., & Guan, Y. (2014) Combined effects of the Pacific decadal oscillation and El Nino-southern oscillation on global land dry–wet changes. *Scientific reports*, 4, srep06651. https://doi.org/10.1038/srep06651.

Ward, P.J., Beets, W., Bouwer, L.M., Aerts, J.C. and Renssen, H. (2010) Sensitivity of river discharge to ENSO. *Geophysical Research Letters*, 37(12), L12402. https://doi.org/10.1029/2010GL043215.

Webber, B.G., Matthews, A.J. and Heywood, K.J. (2010) A dynamical ocean feedback mechanism for the Madden–Julian Oscillation. *Quarterly Journal of the Royal Meteorological Society*, 136 (648), 740–754. https://doi.org/10.1002/qj.604.

Wills, R.C., Armour, K.C., Battisti, D.S. and Hartmann, D.L. (2019) Ocean–atmosphere dynamical coupling fundamental to the Atlantic multidecadal oscillation. *Journal of Climate*, 32(1), 251–272. https://doi.org/10.1175/JCLI-D-18-0269.1.

Wittenberg, A.T. (2009) Are historical records sufficient to constrain ENSO simulations? *Geophysical Research Letters*, 36(12), L12702. https://doi.org/10.1029/2009GL038710.

Wolter, K., & Timlin, M.S. (1993) Monitoring ENSO in COADS with a seasonally adjusted principal component index. *Proc. of the 17th Climate Diagnostics Workshop*, Norman, OK, NOAA/NMC/CAC, NSSL, Oklahoma Clim. Survey, CIMMS and the School of Meteor., University of Oklahoma, 52–57.

Yamazaki, D., Lee, H., Alsdorf, D.E., Dutra, E., Kim, H., Kanae, S. and Oki, T. (2012) Analysis of the water level dynamics simulated by a global river model: a case study in the Amazon River. *Water Resources Research*, 48(9), W09508. https://doi.org/10.1029/2012WR011869.

Yeh, S.W., Cai, W., Min, S.K., McPhaden, M.J., Dommenget, D., Dewitte, B., Collins, M., Ashok, K., An, S.I., Yim, B.Y. and Kug, J.S. (2018) ENSO atmospheric teleconnections and their response to greenhouse gas forcing. *Reviews of Geophysics*, 56 (1), 185–206. https://doi.org/10.1002/2017RG000568.

Yoon, J.H. (2016) Multi-model analysis of the Atlantic influence on Southern Amazon rainfall. *Atmospheric Science Letters*, 17(2), 122–127. https://doi.org/10.1002/asl.600.

Yoon, J.H. and Zeng, N. (2010) An Atlantic influence on Amazon rainfall. *Climate Dynamics*, 34(2–3), 249–264. https://doi.org/10.1007/s00382-009-0551-6.

Zeng, N., Yoon, J.H., Marengo, J.A., Subramaniam, A., Nobre, C.A., Mariotti, A. and Neelin, J.D. (2008) Causes and impacts of the 2005 Amazon drought. *Environmental Research Letters*, 3(1), 014002. https://doi.org/10.1088/1748-9326/3/1/014002.

Zhang, C. (2005) Madden–Julian oscillation. *Reviews of Geophysics*, 43(2), RG2003. https://doi.org/10.1029/2004RG000158.

Zhang, L. and Wang, C. (2013) Multidecadal North Atlantic sea surface temperature and Atlantic meridional overturning circulation variability in CMIP5 historical simulations. *Journal of Geophysical Research: Oceans*, 118(10), 5772–5791. https://doi.org/10.1002/jgrc.20390.

Zhang, Y., Wallace, J.M. and Battisti, D.S. (1997) ENSO-like interdecadal variability: 1900–93. *Journal of Climate*, 10(5), 1004–1020. https://doi.org/10.1175/1520-0442(1997)010<1004:ELIV>2.0.CO;2.

Zhang, W., Villarini, G., Vecchi, G.A. and Smith, J.A. (2018) Urbanization exacerbated the rainfall and flooding caused by hurricane Harvey in Houston. *Nature*, 563(7731), 384–388. https://doi.org/10.1038/s41586-018-0676-z.

Zsoter, E., Cloke, H., Stephens, E., de Rosnay, P., Muñoz-Sabater, J., Prudhomme, C. and Pappenberger, F. (2019) How well do operational numerical weather prediction configurations represent hydrology? *Journal of Hydrometeorology*, 20(8), 1533–1552. https://doi.org/10.1175/JHM-D-18-0086.1.

Zulkafli, Z., Buytaert, W., Manz, B., Rosas, C.V., Willems, P., Lavado-Casimiro, W., Guyot, J.L. and Santini, W. (2016) Projected increases in the annual flood pulse of the Western Amazon. *Environmental Research Letters*, 11(1), 014013. https://doi.org/10.1088/1748-9326/11/1/014013.

SUPPORTING INFORMATION

Additional supporting information may be found online in the Supporting Information section at the end of this article.

How to cite this article: Towner J, Cloke HL, Lavado W, *et al.* Attribution of Amazon floods to modes of climate variability: A review. *Meteorol Appl*. 2020;27:e1949. https://doi.org/10.1002/met.1949